ORIGINAL ARTICLE



European Association of Nuclear Medicine Practice Guideline/Society of Nuclear Medicine and Molecular Imaging Procedure Standard 2019 for radionuclide imaging of phaeochromocytoma and paraganglioma

David Taïeb ¹ · Rodney J. Hicks ² · Elif Hindié ³ · Benjamin A. Guillet ⁴ · Anca Avram ⁵ · Pietro Ghedini ⁶ · Henri J. Timmers ⁷ · Aaron T. Scott ⁸ · Saeed Elojeimy ⁹ · Domenico Rubello ¹⁰ · Irène J. Virgolini ¹¹ · Stefano Fanti ⁶ · Sona Balogova ^{12,13} · Neeta Pandit-Taskar ¹⁴ · Karel Pacak ¹⁵

Received: 4 June 2019 / Accepted: 10 June 2019 / Published online: 29 June 2019 © Springer-Verlag GmbH Germany, part of Springer Nature 2019

Abstract

Purpose Diverse radionuclide imaging techniques are available for the diagnosis, staging, and follow-up of phaeochromocytoma and paraganglioma (PPGL). Beyond their ability to detect and localise the disease, these imaging approaches variably characterise these tumours at the cellular and molecular levels and can guide therapy. Here we present updated guidelines jointly approved by the EANM and SNMMI for assisting nuclear medicine practitioners in not only the selection and performance of currently available single-photon emission computed tomography and positron emission tomography procedures, but also the interpretation and reporting of the results. **Methods** Guidelines from related fields and relevant literature have been considered in consultation with leading experts involved in the management of PPGL. The provided information should be applied according to local laws and regulations as well as the availability of various radiopharmaceuticals.

Conclusion Since the European Association of Nuclear Medicine 2012 guidelines, the excellent results obtained with gallium-68 (⁶⁸Ga)-labelled somatostatin analogues (SSAs) in recent years have simplified the imaging approach for PPGL patients that can also be used for selecting patients for peptide receptor radionuclide therapy as a potential alternative or complement to the traditional theranostic approach with iodine-123 (¹²³I)/iodine-131 (¹³¹I)-labelled meta-iodobenzylguanidine. Genomic

This article is part of the Topical Collection on Oncology - General

- ☐ David Taïeb david.taieb@ap-hm.fr
- Department of Nuclear Medicine, La Timone University Hospital, CERIMED, Aix-Marseille University, 264 rue Saint-Pierre, 13005, Marseille Cedex 05, France
- Centre for Cancer Imaging, Peter MacCallum Cancer Centre, Melbourne, VIC, Australia
- Department of Nuclear Medicine, Hôpital Haut-Lévêque, Bordeaux University Hospitals, Pessac, France
- Department of Radiopharmacy, La Timone University Hospital, CERIMED, Aix-Marseille University, Marseille, France
- Nuclear Medicine/Radiology, University of Michigan, Ann Arbor, MI, USA
- Nuclear Medicine Unit, Medicina Nucleare Metropolitana, University Hospital S.Orsola-Malpighi, Bologna, Italy
- Department of Endocrinology, Radboud University Nijmegen Medical Centre, Nijmegen, The Netherlands
- ⁸ John Hopkins Hospital, Baltimore, MD, USA

- Department of Radiology, University of New Mexico, Albuquerque, NM, USA
- Department of Nuclear Medicine, Radiology, Neuroradiology, Medical Physics, Clinical Laboratory, Microbiology, Pathology, Transfusional Medicine, Santa Maria della Misericordia Hospital, Rovigo, Italy
- Department of Nuclear Medicine, Medical University Innsbruck, Anichstrasse 35, 6020 Innsbruck, Austria
- Department of Nuclear Medicine, Comenius University and St. Elisabeth Oncology Institute, Heydukova 10, 81250 Bratislava, Slovakia
- Department of Nuclear Medicine, Hôpital Tenon Assistance Publique-Hôpitaux de Paris and Sorbonne University, Paris, France
- Department of Radiology, Molecular Imaging and Therapy Service, Memorial Sloan Kettering Cancer Center, New York, NY, USA
- Eunice Kennedy Shriver National Institutes of Child Health and Human Development, National Institutes of Health, Bethesda, MD, USA



Abbroviations

characterisation of subgroups with differing risk of lesion development and subsequent metastatic spread is refining the use of molecular imaging in the personalised approach to hereditary PPGL patients for detection, staging, and follow-up surveillance.

Keywords Guidelines · Radionuclide imaging · Phaeochromocytoma · Paraganglioma · Targeted radionuclide therapy · Positron emission tomography · Somatostatin analogues

Abbreviations		
AADC	Aromatic L-amino acid decarboxylase	
BAT	Brown adipose tissue	
CI	Confidence interval	
CTAC	CT-based attenuation correction	
CT	Computed tomography	
COMT	Catechol-O-methyltransferase	
DA	Dopamine	
DOPA	Dihydroxyphenylalanine	
DTPA	Diethylenetriaminepentaacetic acid	
EGLN1	egl-9 family hypoxia inducible factor 1α	
EGLN2	egl-9 family hypoxia-inducible factor 2α	
EPAS1/HIF2A	Endothelial PAS domain protein 1/	
	hypoxia-inducible factor 2α	
EANM	European Association of Nuclear	
	Medicine	
EPI	Epinephrine	
FH	Fumarate hydratase	
GEP	Gastroenteropancreatic	
GI	Gastrointestinal	
GIST	Gastrointestinal stromal tumour	
HNPGL	Head and neck paraganglioma	
5HT	5-hydroxytryptamine	
MAX	Myc-associated factor X	
MEN	Multiple endocrine neoplasia	
MIBG	Meta-iodobenzylguanidine	
MRI	Magnetic resonance imaging	
MTC	Medullary thyroid carcinoma	
NE	Norepinephrine	
NET	Neuroendocrine tumour	
NF1	Neurofibromin 1	
NPV	Negative predictive value	
PET	Positron emission tomography	
PGL	Paraganglioma	
PHD 1/2	Prolyl hydroxylase 1/2	
PPGL	Phaeochromocytoma and	
	paraganglioma	
PHEO	Phaeochromocytoma	
PPV	Positive predictive value	
PRRT	Peptide receptor radionuclide therapy	
RET	Rearranged during transfection proto-	
P.CC	oncogene	
RCC	Renal cell carcinoma	
SDH	Succinate dehydrogenase	

SDHA, -B, -C, -D	Succinate dehydrogenase		
	subunits A, B, C, and D		
SDHx	Succinate dehydrogenase subunits		
SNMMI	Society of Nuclear Medicine and		
	Molecular Imaging		
SPECT	Single-photon emission		
	computed tomography		
SSAs	Somatostatin analogues		
SSTa	Somatostatin agonist		
SSTR	Somatostatin receptor		
SSTR1, -2, -3, -4, -5	Somatostatin receptor subtypes		
	1, 2, 3, 4, and 5		
SUV	Standardised uptake value		
TLC	Thin-layer chromatography		
TMEM127	Transmembrane protein 127		
VHL	von Hippel-Lindau		
VMAT	Vesicular monoamine transporter		
WHO	World Health Organization		
	-		

Purpose

The aims of the guidelines presented in this article are as follows:

- To assist nuclear medicine practitioners in understanding the role and challenges of radionuclide imaging for PPGLs
- To provide practical information for performing different imaging procedures for these tumours
- 3. To provide an algorithm for selecting the most appropriate imaging procedure in specific clinical situations

Preamble

The Society of Nuclear Medicine and Molecular Imaging (SNMMI) is an international scientific and professional organisation founded in 1954 to promote the science, technology, and practical application of nuclear medicine, while the European Association of Nuclear Medicine (EANM) is a professional non-profit medical association that facilitates communication among individuals pursuing clinical and research excellence in nuclear medicine worldwide. EANM was founded in 1985. SNMMI and EANM members are



physicians, technologists, and scientists specialising in the research and practice of nuclear medicine.

Both SNMMI and EANM periodically define new guidelines for nuclear medicine practice in order to advance the science of nuclear medicine and improve the quality of services offered to patients worldwide. Existing practice guidelines are reviewed for revision or renewal every 5 years or earlier, if indicated.

Each practice guideline, which represents a policy statement released by SNMMI/EANM, is based on a thorough consensus process and extensive review. The societies recognise that the safe and effective use of diagnostic nuclear medicine imaging requires specific training, skills, and techniques, as described in each document. Reproduction or modification of the published practice guideline by entities not providing these services is not authorised.

These guidelines are educational tools designed to assist practitioners in the provision of appropriate care to patients. They are not inflexible rules or requirements of practice and should not be used for establishment of a legal standard of care. For these reasons and those set forth below, both SNMMI and EANM caution against the use of these guidelines in litigation where the clinical decisions of a practitioner are called into question.

The ultimate judgment regarding the propriety of any specific procedure or course of action must be made by the physician or medical physicist in light of all the circumstances presented. Thus, there is no implication that a stand-alone approach differing from the approaches described in the guidelines is below the standard of care. On the contrary, a conscientious practitioner may responsibly adopt a course of action different from that set forth in the guidelines if, as per reasonable judgment, it is indicated because of the condition of the patient, limitations in available resources, or advances in knowledge or technology subsequent to publication of the guidelines.

The practice of medicine includes both the art and the science of prevention, diagnosis, alleviation, and treatment of disease. Because of the variety and complexity of human conditions, it is not always possible to establish the most appropriate diagnosis or predict a particular response to treatment with certainty. Therefore, it should be recognised that adherence to these guidelines will not ensure an accurate diagnosis or a successful outcome. The sole purpose of these guidelines is to ensure that the practitioner delivers effective and safe medical care by following a reasonable course of action based on current knowledge, available resources, and patient needs.

Background information and definitions

Tumour origin and location

Phaeochromocytoma (PHEO) and paraganglioma (PGL), also referred to as PPGL, belong to the same family of neural crest-

derived neoplasms. The reported prevalence of PPGLs varies between 0.2 to 0.6% in patients with hypertension and nearly 5% in patients with an incidentally discovered adrenal tumor [1]. Although the affected sites are widely distributed from the skull base to the pelvis, these tumours almost uniquely develop in close relationship with the sympathetic and parasympathetic divisions of the autonomic nervous system. The sympathetic axis includes the adrenal medulla and chromaffin cells located in the posterior mediastinum (periaortic regions) or retroperitoneum, while the parasympathetic paraganglia are located primarily in the head and neck region and anterior/ middle mediastinum. The term PGL is used to describe extra-adrenal tumours, regardless of their location (sympathetic or parasympathetic). According to the classification by the World Health Organization (WHO), the term PHEO should be reserved solely for adrenal PGL [2].

Clinical presentation

PHEO accounts for approximately 7% (1.5–14%) of all adrenal incidentalomas [3]. However, considering the higher prevalence in autopsy series, these tumours are likely to be underdiagnosed during life. PHEOs usually cause symptoms of catecholamine oversecretion, such as sustained or paroxysmal elevations in blood pressure, headache, episodic profuse sweating, palpitations, pallor, and apprehension or anxiety. In contrast, head and neck PGLs (HNPGLs) are often discovered incidentally during imaging studies or revealed by symptoms and signs of compression or infiltration of adjacent structures, such as hearing loss, tinnitus, dysphagia, and cranial nerve palsies.

Spectrum of hereditary syndromes

Approximately 5–10% of solitary PHEOs are hereditary, whereas the presence of multiple PHEOs or the combination of PHEO with a synchronous or metachronous extra-adrenal PGL is associated with germline/somatic mutations in more than 70% of cases. These are now recognised to be caused by at least 16 susceptibility genes [4].

The most important correlations between the involved gene(s) and specific anatomical predispositions for the tumours have been found as described below.

PHEO: rearranged during transfection proto-oncogene (*RET*), von Hippel–Lindau (*VHL*), succinate dehydrogenase (*SDH*) subunits (*SDHx*), neurofibromin 1 (*NF1*), mycassociated factor X (*MAX*), transmembrane protein 127 (*TMEM127*), and endothelial PAS domain protein 1 (*EPASI*)/hypoxia-inducible factor 2α (*HIF2A*).

Sympathetic PGLs: *SDHx, VHL, EPAS1/HIF2A* and prolyl hydroxylase 1/2 (*PHD1/2*) mutations.

HNPGL: SDHx.

The major predictors of hereditary PPGL include a family history of PPGL, characteristic syndromic presentation, young



age at diagnosis, previous personal history of PPGL, multifocality, an unusual location (e.g. heart, urinary bladder), and/or tumour recurrence, particularly in the adrenal gland, with elevation of normetanephrine and 3-methoxytyramine levels [5, 6]. Renal cell carcinoma (RCC), gastrointestinal stromal tumour (GIST), pituitary adenoma, and, rarely, pulmonary chondroma, neuroblastoma, and neuroendocrine neoplasms (carcinoids) can also be related to *SDHx* mutations [7–9]. Some other manifestations suggestive of certain gene mutations are as follows: prior medullary thyroid carcinoma (MTC), *RET*; café-au-lait spots/neurofibromas, *NF1*; RCC (RCC)/haemangioblastoma/pancreatic tumour, *VHL*; congenital polycythaemia and duodenal somatostatinoma, *EPAS1/HIF2A*; and RCC/leiomyoma, fumarate hydratase (*FH*) (Table 1).

Furthermore, PPGLs with an underlying mutation in *SDH* subunit B (*SDHB*) are associated with a higher risk of aggressive behaviour that may lead to death, particularly due to the development of metastatic disease. The risk of malignancy in *SDHB* mutation-associated tumours has been estimated to range from 31% to 71%. In addition to affecting the disease distribution, the genomically distinct subgroups of PPGLs exhibit different patterns of catecholamine secretion and cell membrane receptor and transporter expression. This influences their imaging phenotype, particularly the uptake of catecholamines or their precursors [10].

Clinical indications for nuclear imaging

Confirmation of a PPGL diagnosis

For confirmation of a PPGL diagnosis, elevated plasma or urinary metanephrines must be observed in addition to clinical symptoms that strongly suggest the presence of these tumours (e.g. sweating, palpitations, hypertension). Plasma or urinary metanephrine levels that are four times the upper reference limit are strongly diagnostic and generally preclude the requirement of other confirmatory tests, with the exception of cases where the patient is taking anti-depressants, which require the clonidine suppression test [11, 12]. Although the medication can be discontinued, it is rarely feasible in clinical practice. Therefore, if biochemical tests indicate the presence of PPGLs, their localisation should follow, generally by anatomical imaging as the first modality. If the metanephrine level is increased, PHEO (an adrenal tumour) should be suspected. If the normetanephrine level is increased, a tumour located in any part of the body should be suspected, and whole-body imaging should be performed. Some specific computed tomography (CT)/magnetic resonance imaging (MRI) features that suggest the presence of PPGL have been reported previously [13]. Typically, PPGLs show soft tissue attenuation that is greater than 10 Hounsfield units (HU) on CT [14]. They also demonstrate avid enhancement on CT and MRI, often with a heterogeneous appearance due to cystic, necrotic, or degenerative changes. In T2-weighted MRI, the classical homogeneous "light-bulb" sign is rarely observed, with heterogeneous enhancement and an intermediate or a high signal intensity being more common. Anatomical imaging is sufficient for the confirmation of PPGL only if the adrenal gland is the site of involvement and the metanephrine level is very high. In this context, it should be noted that almost 99% of epinephrine and, consequently, metanephrine is derived from the adrenal gland. On the other hand, because norepinephrine (NE)/normetanephrine is derived from the adrenal gland or sympathetic nerves present anywhere in the body, functional imaging is required to confirm whether the tumour is indeed PPGL. Differential diagnoses must include other tumours (e.g. neuroblastoma, ganglioneuroma, and composite tumours) and metastatic disease (e.g. lymph node metastasis in patients with a history of PPGL).

Staging at initial presentation of PPGL

Although most PPGLs are benign, approximately 10–20% are thought to be metastatic [4]. Approximately 10–15% of patients with PPGL exhibit metastatic disease at the initial presentation [15]. There are currently some important factors that are either well proven or considered important for the presence of metastatic disease; these include SDHB and alpha thalassemia/mental retardation syndrome X-linked mutations, large tumours (>5 cm), extra-adrenal location, a noradrenergic biochemical phenotype, and, perhaps, a high methoxytyramine level [16-20]. As mentioned above, functional whole-body imaging is preferable for all patients with these characteristics. The caveat is the lack of knowledge about pre-operative genetic testing in most patients. In fact, improvements in current genetic tests and their low cost have significantly reduced the time before which the results are available to clinicians. With regard to HNPGLs, these tumours are often multifocal and occasionally aggressive; therefore, detailed anatomical assessment that includes correlation with the arterial and venous phases of CT or MRI is necessary.

Restaging and follow-up

Restaging and follow-up of these tumours can involve either whole-body CT/MRI or whole-body functional imaging. This is particularly important for patients with specific tumour characteristics that can increase the metastatic potential (as described above). These patients require a lifetime follow-up schedule that generally involves annual metanephrine measurements and whole-body imaging every 2–3 years. Nuclear imaging plays an important role because it is more sensitive than anatomical imaging [21]. It is very specific for PPGL, locates these tumours in unusual locations such as the urinary bladder or heart, and can identify patients who could



Table 1 Characteristics of the various hereditary forms of phaeochromocytomas and paragangliomas

	First manifestation	Context at presentation (in index cases)	PHEO at presentation	Additional extra-adrenal PGL	Biochemical phenotype	Malignancy risk	Other tumour types
MEN2	MEN2 MTC	Adult Possible phenotypic features of MEN2 Family history of MTC/PHEO	Uni- or bilateral	Very rare	ЕРІ	Very low	Parathyroid adenoma/hyperplasia (MEN2A)
NFI	Neurofibromas	Adult Phenotypic features of neurofibromatosis type 1 Family history of neurofibromatosis type 1	Often unilateral	Very rare	ЕРІ	Very low	Peripheral nerve sheath tumours, optical glioma ^a
MAX	MAX PHEO	Young adult Family history of PHFO is common	Bilateral	Uncommon	EPI and NE	Moderate	Renal oncocytoma
VHL	VHL PHEO/PGL	Young adult Family history of DDGI is common	Uni- or bilateral	Moderate (retroneritoneum)	NE	Low	Multiple ^b
SDHA	SDHA PHEO/PGL	Adult Family history of PPGL is extremely	Rare	Moderate (retroperitoneum NE and/or DA or head and neck)	NE and/or DA	Moderate/high GIST °, RCC	GIST °, RCC
SDHB	SDHB PHEO/PGL	rare Adult Econily biotomy of PDCI is massible	Often unilateral	Common (retroperitoneum) NE and/or DA	NE and/or DA	High	GIST ^c , pituitary adenoma, RCC
SDHD	SDHD PHEO/PGL	raffing instead of real is possible Adult Family history of HNDGI is common	Uni- or bilateral	Common (head and neck) NE and/or DA	NE and/or DA	Moderate	GIST°, pituitary adenoma, RCC
SDHC	SDHC PHEO/PGL	Adult Romily, history, of DUEO/DGI is noted	Rare	Common (mediastinum)	NE	Low/Moderate GIST, RCC	GIST, RCC
HIF2A	HIF2A Polycythaemia (often at birth or in early childhood)	Family history of PPGL is absent	ı Rare	Expected (retroperitoneum) NE	NE	High	Somatostatinoma

MAX: myc-associated factor X, MEN: multiple endocrine neoplasia, NF1: neurofibromin 1, VHL: von Hippel-Lindau, SDHA, -B, -C, and -D: succinate dehydrogenase subunits A, B, C, and D, HIF2A: hypoxia-inducible factor 2α, PPGL: phaeochromocytoma and paraganglioma, PHEO: phaeochromocytoma, PGL: paraganglioma, MTC: medullary thyroid carcinoma, HNPGL: head and neck paraganglioma; GIST: gastrointestinal stromal tumour, RCC: renal cell carcinoma, EPI: epinephrine, NE: norepinephrine, DA: dopamine



^a NF1-associated PGEOs/PGLs are characterised by the presence of multiple neurofibromas, café-au-lait spots, Lisch nodules of the iris, and other rare disorders

b VHL disease is an autosomal dominant disorder that also predisposes to renal tumours and clear cell carcinoma, pancreatic serous cystadenomas, pancreatic neuroendocrine tumours, testicular tumours, and haemangioblastoma of the eye and central nervous system

c Non-KIT/PDGFRA GISTs may be caused by mutations in the SDHA-D genes and could be associated with PGLs in patients with Camey-Stratakis syndrome

^d HIF2A-related PHEOs/PGLs are associated with the presence of duodenal somatostatinoma and retinal abnormalities (Pacak–Zhuang syndrome)

benefit from radiotherapy. Furthermore, PPGL-specific functional imaging is minimally influenced by the post-treatment sequelae, thus enabling accurate diagnosis of tumour recurrence/metastasis that could be missed by anatomical imaging [22]. Finally, this imaging modality is also very useful for the assessment of responses to therapies in cases of metastatic or inoperable PPGL.

Selection for targeted molecular radiotherapy

Recently, the success of peptide receptor radionuclide therapy (PRRT) with lutetium-177 (¹⁷⁷Lu)-labelled DOTA-Tyr3-octreotate (DOTATATE; oxodotreotide) or other yttrium-90 (⁹⁰Y)- or ¹⁷⁷Lu-labelled somatostatin analogues (SSAs) in patients with inoperable/metastatic gastroenteropancreatic (GEP) neuroendocrine tumours (NETs) has provided a great impetus toward its use for inoperable/metastatic PPGL.

Nuclear imaging (PET or SPECT) provides valuable information when planning targeted radionuclide therapy with iodine-131 (¹³¹I)-labelled meta-iodobenzylguanidine (MIBG) or PRRT with [¹⁷⁷Lu]-labelled DOTATATE (currently used for PPGL in the setting of research or compassionate treatment programs) or other related agents [23]. In addition to confirming the lesion uptake, it helps in personalised dosimetric evaluation of at-risk organs and tumour targets.

Radiotherapy planning

Nowadays, integration of multimodal imaging into radiotherapy planning has increased the precision of radiation delivery. Molecular imaging can complement MRI in difficult situations, particularly evaluations of venous extensions from large jugular PGLs or tumour recurrences in the surgical bed; therefore, it could lead to a more accurate definition of biological target volumes and potentially decrease the likelihood of complications within the surrounding normal tissues. This is particularly true for stereotactic radiosurgery, which enables the delivery of a very high biologically effective dose to the tumour.

Useful clinical information for optimal imaging and interpretation

A nuclear medicine physician should obtain the following information whenever possible.

- 1. Personal history of PPGL and/or other tumours
- Personal history of surgery, chemotherapy, and radiotherapy (including timing and frequency)
- Known genetic mutations or documented family history of PPGL
- 4. Results of PPGL-related laboratory tests (metanephrines, methoxytyramine, calcitonin, chromogranin A levels)

- Results of previous anatomical and functional imaging studies, including baseline and nadir on-treatment imaging for the assessment of the tumour response(s)
- 6. Use of drugs (e.g. proton pump inhibitors, histamine type-2 receptor antagonists) or the presence of conditions (gastric disorders, impaired renal function, chronic heart failure, hypertension, rheumatoid arthritis, inflammatory bowel disease, non-neuroendocrine neoplasms) that may interfere with the accuracy of procedures and measurements (particularly for chromogranin A)

General considerations for image acquisition and interpretation are outlined as follows.

- PPGLs have different preferential sites of origin that must be known. The integration of functional and anatomical imaging in hybrid SPECT/CT or PET/CT devices is strongly recommended.
- Images are generally acquired from the top of the skull (for a large jugular PGL) to the pelvis. In cases where recurrent or metastatic disease is suspected, whole-body images are necessary.
- Malignancy is defined only by the presence of metastases at sites where chromaffin cells are normally absent. According to the current 2017 WHO Classification of Tumours of Endocrine Organs, these sites include only bones and lymph nodes.
- 4. The presence of retroperitoneal PGLs or multifocal tumours increases the possibility of hereditary syndromes and requires extensive searches for additional PPGLs and other syndromic lesions, most commonly GIST, RCC, pancreatic tumour, haemangioblastoma, MTC, pituitary adenoma, neuroblastoma, and/or somatostatinoma.
- All non-physiological and suspicious foci of tracer uptake must be described, considering PGLs may arise in various atypical locations such as the orbits, thyroid gland, hypoglossus muscle, heart, pericardium, gallbladder, urinary bladder, liver, and cauda equina.
- 6. Metastases from PPGLs are often small and numerous and could be difficult to localise precisely on coregistered CT images obtained by combined SPECT/CT and PET/CT (plain CT, thick anatomical sections, or a positional shift between CT and nuclear images).

General points to consider for reporting are outlined as follows.

- 1. The clinical setting and clinical question
- 2. Details of patient preparation, including withheld concomitant drugs
- Procedure details, including the radiopharmaceutical agent; administered activity; injection site; acquisition protocol; CT parameters in case of hybrid imaging;



- radiation exposure, including the effective dose resulting from administration of the radiopharmaceutical; and CT parameters related to the radiation dose, including the volume computed tomography dose index and doselength product
- Positive findings and interpretation for each anatomical region, i.e. the head and neck, chest, abdomen and pelvis, and bone/bone marrow
- Data comparisons with other imaging studies or previous nuclear imaging studies

Conclusions

The report should present findings in terms of their compatibility with a particular diagnosis, followed by a list of study limitations. When conclusive evidence requires additional diagnostic functional or morphological examinations or an adequate follow-up schedule, the same should be mentioned in the report. The feasibility of radionuclide therapy should be mentioned in cases of metastatic disease. Genetic testing could be suggested if a hereditary syndrome, family history, or multiplicity is suspected or found.

[123 I]lobenguane/[123 I]MIBG scintigraphy

Radiopharmaceutical

Commercially available MIBG is radiolabelled with ¹²³I or ¹³¹I. [¹²³I]MIBG scintigraphy is strongly preferred over [¹³¹I]MIBG scintigraphy for various reasons. First, it provides images of superior quality, because 159-keV emission of ¹²³I is better adapted to detection with conventional gamma cameras. Second, the lower radiation burden of ¹²³I allows higher permissible administered activity, which results in a higher count rate. Third, SPECT is easier to perform with ¹²³I. Fourth, the time between injection and imaging is shorter with [¹²³I]MIBG scintigraphy (24 h) than with [¹³¹I]MIBG scintigraphy (48–72 h).

Mechanism of cellular uptake

MIBG, an iodinated guanidine analogue, is structurally similar to NE. Guanidine analogues and NE share a common transport pathway via the cell membrane NE transporter system. Non-specific MIBG uptake in PPGL tissues has also been reported [24, 25]. In the cytoplasmic compartment, MIBG is stored in the neurosecretory granules via vesicular monoamine transporters (VMAT) 1/2 [26]. Moreover, it specifically concentrates in catecholamine-secreting tissues and tumours, allowing their specific detection.



Pharmacokinetics

After intravenous administration, MIBG concentrates in the liver (33%), lungs (3%), heart (0.8%), spleen (0.6%), and salivary glands (0.4%) [27]. A small amount of the remaining MIBG concentrates in platelets through the serotonin or 5-hydroxytryptamine (5HT) transporter. Tracer uptake in the normal adrenal glands is weak and facilitates faint visualisation, particularly when [123 I]MIBG is used. The majority of MIBG [27] is excreted in unaltered form by the kidneys (70–90% of the injected dose is eliminated in the urine within 4 days after administration, with 50% eliminated within the first 24 h), with minor amounts eliminated in the faeces (<2% up to day 4). In patients with PPGL, uptake in the heart and liver is lowered by approximately 40%, most likely as a consequence of competition with circulating catecholamines [28].

Synthesis and quality control

[¹²³I]MIBG or [¹³¹I]MIBG is commercially available as a ready-to-use formulation that conforms to European/United States (US) pharmacopoeia requirements. It is packaged as a sterile solution for intravenous use. The solution is colourless or slightly yellow, contains 0.08 mg/ml of iobenguane sulfate, remains stable for 36 h after the calibration time, and can be diluted in sterile water or saline. The activity of MIBG should be measured in a calibrated ionisation chamber, while the radiochemical purity can be evaluated using thin-layer chromatography (TLC).

Drug interactions

Many drugs modify the uptake and storage of MIBG and may interfere with MIBG scintigraphy [29]. It should be underlined that most of the therapeutic pharmaceuticals introduced in the last 25 years and in common use today have never been tested for their effects on MIBG uptake [30, 31]. Reported interfering agents include opioids, tricyclic or other anti-depressants, sympathomimetics, anti-psychotics, and some anti-hypertensive agents [32–34]. Labetalol, for example, has been reported to cause false-negative results and should be discontinued for more than 10 days before MIBG administration, if the patient's clinical condition permits [35, 36]. In one study, a single oral dose of amitriptyline, a tricyclic anti-depressant, significantly enhanced cardiac MIBG washout and competed with catecholamines on the norepinephrine transporter, resulting in low MIBG accumulation in PPGLs [37]. Another report documented that post-treatment MIBG scintigraphy failed to detect the vast majority of metastatic PPGL lesions in a patient with polytoxicomania who exhibited a positive diagnostic scan [38]. Nifedipine, on the other hand, can cause prolonged MIBG retention in PPGLs [39]. Calcium antagonists are generally listed as medications that interfere with MIBG uptake, although definitive proof is lacking. In all probability, it may not be necessary to withdraw them [30]. Very high serum catecholamine levels may be associated with lower MIBG accumulation [40–43]. To date, many of these interactions are suspected on the basis of in vitro/preclinical observations or simply anticipated on the basis of their pharmacological properties; thus, they should be interpreted with caution. Furthermore, mechanisms involved in MIBG uptake or retention may differ between models. For example, specific MIBG uptake is mediated by the 5HT transporter in platelets and NE transporter in PPGLs.

Side effects

- Rare adverse events (tachycardia, pallor, vomiting, abdominal pain) can be prevented by slow injection.
- No adverse allergic reaction is expected, although a single case of allergy caused by [¹³¹I]MIBG has been reported [44].

Recommended activity

In adults, the recommended activity for [¹²³I]MIBG is 370 MBq for a body weight of 70 kg, while that for [¹³¹I]MIBG is 40–80 MBq. In children, the administered activity should be scaled according to the body weight. For [¹²³I]MIBG, the recommended activity is 5.2 MBq/kg, with minimum activity of 37 MBq and maximum activity of 370 (North America) or 400 (Europe) MBq. For [¹³¹I]MIBG, the recommended activity is 35–78 MBq [34].

Administration

Slow intravenous injection over at least 1 min is recommended.

Radiation dosimetry

The effective [123I]MIBG and [131I]MIBG doses are 0.013 and 0.14 mSv/MBq, respectively, for adults, and 0.037 and 0.43 mSv/MBq, respectively, for children (5 years) [45]. CT delivers an additional radiation dose in SPECT/CT protocols, with the value being dependent on the scanning parameters.

Pregnancy

The use of radiopharmaceuticals is generally contraindicated in pregnancy. However, if clinically necessary, a decision to perform imaging in cases of known or suspected pregnancy should be based on an analysis of the benefits versus the possible risks to the foetus. Proper institutional and local guidelines should be followed.

Breastfeeding

Breastfeeding should be discontinued for at least 3 days after [¹²³I]MIBG administration without contamination by [¹²⁴I] or [¹²⁵I]. When [¹³¹I]MIBG is used, breastfeeding should be stopped completely.

Renal insufficiency

Reduced plasma clearance of [¹²³I]MIBG occurs in patients with renal insufficiency. [¹²³I]MIBG is not dialysable [46]. Therefore, a reduction in the administered activity by 50% and possible delayed imaging should be considered.

Patient preparation

- For [123 I]MIBG, thyroid blockade (administration of potassium iodide 130 mg/day; equivalent to 100 mg of iodine) should be performed 1 h (30 min to 2 h) before tracer injection. For diagnostic use of [131 I]MIBG, blockade should be initiated 24 h before tracer injection and continued daily for at least 5 days after injection. However, the use of this agent for diagnostic imaging is strongly discouraged [47]. Potassium perchlorate may be used as a substitute for Lugol's iodine in patients with iodine allergy; it should be administered 4 h before tracer injection and continued for 2 days after injection (400–600 mg/day).
- Drugs that can interfere with MIBG uptake and retention (opioids, tricyclic or other anti-depressants, sympathomimetics, and anti-hypertensive agents, particularly combined alpha and beta adrenoreceptor antagonists and calcium antagonists) should be discontinued for 1–3 days. An exception is labetalol, which should be discontinued 10 days before the procedure. Anti-psychotics should be withdrawn for approximately 3–4 weeks; however, their withdrawal can prove dangerous and should be implemented only after thorough consultation with the patient's psychiatric care team.
- Decisions to discontinue other medications should be in accordance with the clinical setting and closely coordinated with the managing clinician.

Image acquisition and reconstruction

In [123I]MIBG scanning, images should be obtained approximately 24 h after tracer injection.

Imaging parameters

Anterior and posterior planar static images of the head and neck (plus right and left lateral oblique views), thorax,



abdomen, and pelvis are obtained for 10-15 min per image (or approximately 500 kcounts). A 256×256 matrix, large-field-of-view camera, low-energy collimator, and 20% window centred at the 159-keV photopeak are used. Whole-body images can be an alternative to planar views and include anterior and posterior acquisitions with a 1024×512 or 1024×256 matrix size and a minimum imaging duration of 30 min (maximum speed, 6 cm/min) [32].

Some centres prefer collimators with medium energy because they reduce scatter and septal penetration of high-energy photons that are part of the ¹²³I decay scheme. However, longer acquisition times are required with medium-energy collimators.

SPECT or SPECT/CT over the anatomical regions showing pathological tracer uptake on planar images often complete the imaging session and can replace lateral and oblique planar images of the head and neck region. The SPECT images are acquired for a 360° orbit (128 × 128 matrix, 6° angle steps, 30–45 s per stop). Co-registered CT images (100–130 kV, mA modulation recommended) obtained from SPECT/CT cameras enable attenuation and facilitate precise localisation of all foci with increased tracer uptake.

Reconstruction

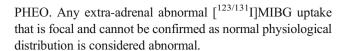
Iterative SPECT reconstruction or other validated reconstruction protocols that allow accurate lesion visualisation can be adapted to the clinical setting. CT-based attenuation correction (CTAC) is used for SPECT/CT.

Image interpretation

Visual analysis

Physiological distribution Normal uptake of [123 I]MIBG is observed in the following organs: myocardium, salivary glands, lacrimal glands, thyroid gland, liver, lungs, adrenal glands (in up to 80% of cases), bowel, and uterus (during menstruation). It should be noted that [123 I]MIBG uptake in the adrenal glands is considered normal if it is mild (lower than or equal to the liver uptake) and symmetrical, and if the glands are not enlarged on CT images. High intestinal activity may also be observed. In some patients with PPGL, brown adipose tissue (BAT) is activated by high norepinephrine levels; consequently, [123/131 I]MIBG uptake can be detected in BAT and should be considered normal. The sole use of beta-adrenoceptor blockers for lowering the BAT uptake (as indicated for other patients, including those with various cancers) is contraindicated in patients with PPGL.

Pathological uptake Increased or asymmetrical uptake of [123/131]]MIBG in the presence of an enlarged adrenal gland is considered abnormal and often suggests the presence of



Quantification

Quantification of the MIBG uptake is not routinely performed, because of the lack of well-established methodology. Quantitative SPECT/CT has been developed to facilitate dosimetry for therapeutic radionuclides, including ¹⁷⁷Lu [48, 49]; however, it can be used in routine clinical practice only after thorough validation [50].

Common pitfalls

False-positive findings

CT-based attenuation correction often leads to enhanced physiological visualisation of the adrenal medulla, sometimes resulting in false-positive findings/conclusions. In cases where adrenomedullary hyperplasia precedes PHEO development (e.g. those associated with SDHx or MEN2), [123] MIBG scintigraphy may initially be of limited value for discriminating diffuse adrenal medullary hyperplasia from true PHEO. False-positive findings are also caused by other tumours that express the NE transporter system on the cell membrane; these include carcinoids, MTC, Merkel cell carcinoma, ganglioneuroma, and composite tumours. Abnormally increased MIBG uptake in adrenocortical adenomas or carcinomas, retroperitoneal angiomyolipomas and haemangiomas, and some GEP NETs has been rarely reported. The use of SPECT/CT often prevents false interpretation of abnormal MIBG accumulation in the liver (e.g. hepatic haemangioma, hepatocellular carcinoma), renal parenchyma (e.g. diffuse accumulation in renal artery stenosis and focal accumulation in acute pyelonephritis), and urinary tract (hydronephrosis, renal cysts); atelectasis; pneumonia; vascular malformations; accessory spleens; adrenal abscesses; foregut duplication cysts; haemorrhagic cysts; ovarian torsion; and chronic inflammatory foci [34].

False-negative findings

HNPGLs; *SDHx*-associated PPGLs; very small lesions measuring less than 7 mm; PHEOs with cystic degeneration, necrosis, or haemorrhage; and some poorly differentiated PPGLs with low VMAT 1 expression can be associated with falsenegative findings [51–55]. It should be noted that some falsenegative results may also be a consequence of interfering drugs that are often necessary to control hypertension and tachyarrhythmia in patients with PPGLs [11, 56].



Diagnostic accuracy

Initially, according to small-scale studies that mainly included patients with PHEO, the sensitivity and specificity of [123] [MIBG scintigraphy were estimated at 83–100% and 95–100%, respectively. Subsequently, larger studies including large numbers of extra-adrenal, multiple, recurrent, and hereditary PGLs found sensitivity of 52-75% [51, 53-55]. It is currently well known and repeatedly documented that [123] [MIBG scintigraphy should not be used for patients with SDHB-associated PPGLs, less than 50% of which exhibit positivity [52, 57, 58]. This is also true for metastatic PPGLs [51, 55, 59-62]. In cases involving HNPGLs, the sensitivity of ¹²³I-MIBG scintigraphy is lower (18–50%) than that of other functional imaging modalities, particularly those using [⁶⁸Ga]DOTA-SSAs [63]. Nevertheless, [¹²³I]MIBG scintigraphy is very useful for the selection of potential candidates for [¹³¹I]MIBG therapy.

Indium-111 (¹¹¹In)-labelled pentetreotide scintigraphy

Radiopharmaceutical

Pentetreotide is a diethylenetriaminepentaacetic (DTPA) conjugate of octreotide, a long-acting SSA.

Mechanism of uptake

[111In]DTPA-pentetreotide (OctreoScanTM) specifically binds to somatostatin receptors (SSTRs) that are overexpressed on cell membranes, particularly subtypes 2 and 5. SSTRs are expressed on many cells with a neuroendocrine origin and, consequently, tumours derived from those cell types.

Pharmacokinetics

[111In]DTPA-pentetreotide is cleared from the blood, primarily through the kidneys (50% and 85% of the injected dose is recovered in the urine by 6 and 24 h, respectively). However, some of the tracer is retained in the tubular cells. Hepatobiliary excretion and spleen trapping account for 2% and 2.5% of the administered dose, respectively. However, the bowel is often visualised on delayed imaging, and the gallbladder can also contain activity and cause diagnostic uncertainty unless careful correlation with anatomical imaging is performed. The pituitary and thyroid glands can also be visualised [64, 65].

Synthesis and quality control

[111In]DTPA-pentetreotide is commercially available (OctreoScanTM) and supplied as a monodose kit for

radiolabelling. The kit contains two sterile vials containing lyophilised pentetreotide (10 μ g) and indium (¹¹¹I) chloride (122 MBq/1.1 mL at ART).

The radiopharmaceutical is prepared by adding the desired activity of indium (¹¹¹I) chloride into the vial containing pentetreotide at room temperature. The preparation can be diluted in sterile saline (2–3 mL).

The [¹¹¹In]DTPA-pentetreotide preparation remains stable for 6 h and should not be used if the radiochemical purity is less than 90% (USA) or 99% (Europe). The pH of the solution ranges from 3.8 to 4.3.

TLC can be used to check the radiochemical purity as follows: solid phase instant TLC; mobile phase, 0.1 N sodium citrate adjusted with HCl to a pH of 5; Rf, ¹¹¹In-pentetreotide 0.0, unbound ¹¹¹In 1.0.

Drug interactions and side effects

It is recommended that SSA therapy be temporarily discontinued in order to avoid possible SSTR blockade; however, this is not universally applicable.

Recommended activity

185–222 MBq in adults and 3 MBq/kg in children [66].

Administration

Slow intravenous infusion over 1–2 min.

Radiation dosimetry

The effective dose is approximately 0.054 mSv/MBq for adults and 0.16 mSv/MBq for children (5 years) [67]. CT delivers an additional radiation dose in SPECT/CT protocols, with the value being dependent on the scanning parameters.

Renal failure

In patients with significant renal failure, high blood pool activity may impair the visualisation of uptake foci. An interpretable scintigram can be obtained after haemodialysis.

Pregnancy

The use of radiopharmaceuticals is generally contraindicated in pregnancy. A decision to perform imaging in cases of known or suspected pregnancy should be based on an analysis of the benefits versus the possible risks to the foetus.



Breastfeeding

Breastfeeding need not be discontinued after the diagnostic use of [111]DTPA-pentetreotide. However, close contact with infants should be restricted during the first 2 days after injection. Recommendations may, however, vary in different countries.

Patient preparation

- SSAs are rarely used for the treatment of PPGLs. Short-acting SSAs can be discontinued for 24 h before [111In]DTPA-pentetreotide administration, whereas long-acting analogues are preferably withdrawn 4–6 weeks before the study. Alternatively, imaging can be performed just before the next depot injection. If necessary, the treatment should be switched to short-acting formulations [66, 68].
- Laxatives may be considered, particularly when the abdomen is the area of interest. SPECT/CT may obviate the need for pretreatment with laxatives, as it allows better delineation of physiological bowel activity.
- To minimise radiation exposure, patients should be well hydrated before and for at least 1 day after injection.

Image acquisition

· Timing of imaging

Scans are obtained at 4 and 24 h after tracer injection.

- Imaging field
- Images are acquired using two energy peaks at 171 and 245 keV and medium-energy collimators with a large field of view
- Anterior and posterior planar views of the head and neck (plus right and left lateral oblique views), thorax, abdomen, and pelvis are acquired at 4 and 24 h (512 × 512 or 256 × 256 matrix) for 10–15 min per view (or approximately 300 kcounts for the head and neck and 500 kcounts for the rest of the body) [65, 66].
- Whole-body images can be acquired instead of planar views. Anterior and posterior whole-body images are acquired with a 1024 × 512 or 1024 × 256 matrix size for a minimum of 30 min (maximum speed, 6 cm/min).
- SPECT of the anatomical regions showing pathological tracer uptake on planar images is very helpful. The images are acquired for a 360° orbit (128 × 128 matrix, 6° angle steps, 30–45 s per stop). Co-registered CT images (100–130 kV, mAs modulation recommended) obtained from SPECT/CT cameras enable attenuation and facilitate

precise localisation of any foci of increased tracer uptake. SPECT/CT images are particularly useful for the abdominal area. In cases of a single acquisition, the procedure should be performed at 24 h because of a higher target-to-background ratio, even though the bowel activity is higher.

- Optional images
- Acquisitions (SPECT and/or planar views) may be repeated at 48 h for clarification of equivocal abdominal findings.

Reconstruction

Iterative SPECT reconstruction or other validated reconstruction protocols that facilitate accurate lesion visualisation can be adapted to the clinical setting. CTAC is recommended for SPECT/CT.

Image analysis

Visual analysis

Physiological distribution Uptake can be observed in the spleen, kidney, liver, bowel (visible on the 24-h images), and gallbladder. Normal adrenal glands are also faintly visible. Other sites with faint uptake include the pituitary and thyroid glands (increased diffuse uptake in the case of thyroiditis).

Pathological uptake Accumulation of radioactivity at an abnormal site is considered to represent SSTR binding, particularly when observed on the scintigrams acquired at the two standard imaging time points.

Quantification

The optimal time interval for tumour quantification after injection is 24 h or more. Tumour uptake is scored according to the Krenning scale, which takes into account physiological uptake in the liver and spleen as reference organs. A modified Krenning score based on the same reference tissues has also been applied to SPECT, although it is not necessarily equivalent, particularly for small hepatic lesions.

Pitfalls

False-positive findings

Renal parapelvic cysts, accessory splenic tissue, or abdominal hernia can result in false-positive findings. Tracer uptake by NETs or other tumours that express SSTR subtype 2 (SSTR2) should also be considered [66]. Because SSTR2 is also overexpressed in activated lymphocytes and macrophages,



false-positive findings can also be obtained if granulomatous and/or inflammatory diseases are present.

False-negative findings

Small HNPGLs and abdominal PGLs can be associated with false-negative findings.

Diagnostic accuracy

Several previous studies have found that [¹¹¹In]DTPA-pentetreotide scintigraphy is superior to [¹³¹I/¹²³I]MIBG scintigraphy for HNPGLs, with sensitivity of 79–100% and 18–50%, respectively [69–75].

In some studies, [111In]DTPA-pentetreotide scintigraphy was found to provide complementary information to [123I]MIBG scintigraphy for the detection of HN and metastatic PPGLs [53, 76–78]. Many studies have documented that [111In]DTPA-pentetreotide can also detect other tumours, including GEP NET, MTC, neuroblastoma, and pituitary tumours. However, the diagnostic performance of scintigraphy with both of these single-photon agents has been shown to be inferior to that of other PET/CT procedures described below.

PET with [⁶⁸Ga]SSAs

Radiopharmaceuticals

SSTR imaging using PET tracers has been performed with three different DOTA-coupled somatostatin agonists (SSTas), namely DOTA-Tyr3-octreotide (DOTATOC, edotreotide), DOTA-Tyr3-octreotate (DOTATATE, oxodotreotide), and DOTA-Nal3-octreotide (DOTANOC). All of these are radiolabelled with ⁶⁸Ga obtained from ⁶⁸Ge/⁶⁸Ga generators, which have received marketing authorisation worldwide. DOTATATE and DOTATOC were recently approved by the US Food and Drug Administration and European Medicines Agency (EMA), respectively.

Because of the short half-life of ⁶⁸Ga (68 min), [⁶⁸Ga]SSTas are synthesised less than 4 h before injection on the day of examination. According to the country's regulations, the agent can be centrally manufactured and shipped to the respective nuclear medicine departments or synthesised in local radiopharmacies meeting good manufacturing practice guidelines.

Mechanism of cellular uptake

[⁶⁸Ga]SSTas target SSTR2, which is the most common overexpressed receptor in PPGLs and is internalised into the cells. SSTR subtype 1 (SSTR1) is also strongly expressed in some PGLs, whereas the other subtypes are slightly or not

expressed. The low expression of SSTR subtype 5 (SSTR5) in PGLs constitutes a major difference from some NETs involving the gastrointestinal tract. DOTATOC, DOTATATE, and DOTANOC exhibit excellent affinity for SSTR2 (IC50: 2.5 nM, 0.2 nM, and 1.9 nM respectively). DOTANOC also binds specifically to SSTR3, SSTR4, and SSTR5, while DOTATOC binds to SSTR5, albeit with lower affinity than DOTANOC [79–81].

Tracer binding and retention depends on the density of SSTRs on the cell surface and the degree of internalisation of the ligand/receptor complex. SSTR antagonists including [⁶⁸Ga]NODAGA-JR11 [82] have recently been developed and are currently under evaluation. These antagonists are expected to reduce the washout of DOTA-peptides and increase the target residence time despite the lack of internalisation, because these radiopharmaceuticals remain anchored within the cell membrane. According to the theranostic concept, ⁶⁸Ga-radiolabelled antagonists can also be used as theranostic agents [82].

Pharmacokinetics

After intravenous administration, [⁶⁸Ga]SSTas concentrate in all SSTR2-expressing organs; these include the pituitary, thyroid, adrenal, prostate, and salivary glands; spleen; kidney; pancreas; and liver. There is no significant uptake in the cerebral cortex, heart, bones, red marrow, or gastrointestinal tract [83]. [⁶⁸Ga]DOTA-SSTas showed a bi-exponential blood half-life (2 and 50 min) and are mainly excreted by the kidney (40% and 75% of the injected dose at 3 and 24 h after injection, respectively). Less than 2% of the injected dose is excreted in the faeces by 48 h after injection, and no radiolabelled metabolites have been observed during the first 4 h.

Synthesis and quality control

Currently, two ⁶⁸Ge/⁶⁸Ga generators and DOTATOC and DOTATATE have marketing authorisation. ⁶⁸Ga can be obtained from ⁶⁸Ge/⁶⁸Ga generators on a daily basis for several months.

DOTATOC and DOTATATE are available as commercial kits for radiolabelling. ⁶⁸Ga radiolabelling requires 20–30 min and can be performed manually or with the use of automated devices.

Briefly, the labelling procedure is divided into different steps and performed using suitable shielding to minimise radiation exposure.

- ⁶⁸Ga chloride elution: ⁶⁸Ge/⁶⁸Ga generators are eluted with hydrochloric acid solution (0.1–1 N).
- DOTA-conjugated peptide radiolabelling: A defined volume of ⁶⁸Ga eluate and buffer are successively added in aseptic conditions, and the mixture is



- heated (95 °C, 7–8 min) according to the manufacturer's recommendations.
- Purification: If required on the basis of generator characteristics, a purification step using an accessory cartridge can be performed to reduce the amount of ⁶⁸Ge to less than 0.001%. Radionuclidic identity is then mandatory and tested by half-life measurements, gamma-ray spectral analysis, and determination of any long-lived radionuclidic impurities at 24 h after the end of synthesis.
- Quality control: The appearance, pH, and radiochemical purity must be assessed before injection using validated methods such as TLC or high-performance liquid chromatography. The radiochemical purity of [⁶⁸Ga]DOTATATE and [⁶⁸Ga]DOTATOC must be higher than 92% and 95%, respectively. Samples are periodically tested for sterility.

Drug interactions and side effects

Treatment with cold SSAs may affect tracer accumulation in different organs and tumour sites [84].

Recommended activity

For adults, the recommended activity is 2 MBq/kg (100–200 MBq). The administered amount of SSTa should not exceed 40 μg .

Administration

Slow intravenous infusion over 1–2 min.

Radiation dosimetry

The effective radiopharmaceutical dose for adults is approximately 0.021 mSv/MBq [85]. An additional radiation dose is delivered by CT, with the value being dependent on the scanning parameters.

Pregnancy

The use of radiopharmaceuticals is generally contraindicated in pregnancy. However, if clinically necessary, a decision to perform imaging in cases of known or suspected pregnancy should be based on an analysis of the benefits versus the possible risks to the foetus. Please refer to the section on fluorine-18 (¹⁸F)-labelled fluorodeoxyglucose (FDG) PET for additional details.

Breastfeeding

Breastfeeding should be discontinued for 12 h after injection.



Patient preparation

There is no fasting requirement before injection. According to empirical evidence, it is preferable to perform imaging with [⁶⁸Ga]SSAs on the day(s) preceding the next administration of SSAs. Therefore, discontinuation of short- and long-acting SSAs for 1 day or 3 weeks before imaging with [⁶⁸Ga]SSAs, respectively, is recommended. However, this aspect requires further clarification [86].

Image acquisition

Scans are generally obtained from 45 to 90 min after tracer injection, from the base of the skull to the mid-thighs or for the whole body, depending on the clinical setting. Although there is no generally accepted acquisition time in the literature, 3 min per bed position is considered adequate. However, to minimise the risk of a low-quality scan, the acquisition time per bed position should be increased for obese patients and in cases where low ⁶⁸Ga activity is available or imaging is delayed beyond 90 min.

Image reconstruction

Data may be acquired in the three-dimensional (3D) or twodimensional (2D) mode. Iterative reconstruction algorithms represent the current standard for routine clinical practice. Point spread function algorithms may enhance the detection of small lesions, although they tend to increase the apparent uptake intensity in such structures [87]. This may affect the interpretation of uptake in the adrenal glands.

Image analysis

Visual analysis

Physiological distribution Intense accumulation of radioactivity is seen in the spleen (and accessory splenic tissue if present), kidneys, and adrenal, salivary, and pituitary glands. Accumulation in the liver is generally less intense than that in the spleen. The thyroid is faintly visible. In addition, variable tracer uptake is frequently observed in the pancreas, particularly the uncinate process, because of a higher concentration of pancreatic polypeptide cells [88]. The prostate gland and breast glandular tissue may show diffuse, low-grade uptake of [68Ga]DOTA-SSAs.

Quantification

The Krenning scale is not validated for [⁶⁸Ga]SSTa PET/CT. The standardised uptake value (SUV) is an easy-to-measure and useful parameter for tumour characterisation if images are acquired and processed in a standardised manner. It should be

ensured that the PET/CT system is calibrated for the half-life of ⁶⁸Ga. SUVs in organs differ between various [⁶⁸Ga]SSTa.

Pitfalls

False-positive findings

[⁶⁸Ga]SSTa PET can result in false-positive findings of metastatic lymph nodes due to various cancers, meningioma, inflammatory diseases, the pituitary gland, and some rare conditions such as fibrous dysplasia [89, 90]. Focal pancreatic accumulation in the uncinate process may mimic a pancreatic NET.

False-negative findings

There are insufficient data to draw any firm conclusions. False-negative findings mainly occur in cases involving PHEOs. As observed in PET using other radiopharmaceuticals, the urinary bladder may mask intra- or perivesical PGLs. Diuretics can be used to circumvent this drawback in selected cases.

Diagnostic accuracy

There are scarce data on the use of [68Ga]DOTA-SSA for primary PHEOs/PPGL, although it has shown excellent results in localisation of these tumours when they are metastatic or extra-adrenal [90–95]. Moreover, [68Ga]DOTA-SSA PET has been found to be more sensitive than [123/131] MIBG scintigraphy [96]. In a recent systematic review and meta-analysis, the pooled detection rate for [68Ga]DOTA-SSA PET/CT was 93% [95% confidence interval (CI), 91-95%], which was significantly higher (P < 0.001 for all) than that for [18 F]-labelled fluorodihydroxyphenylalanine (FDOPA) PET/CT (80%; 95% CI, 69-88%), [18F]FDG PET/CT (74%; 95% CI, 46-91%), and [123/131] [MIBG scintigraphy (38%; 95% CI, 20–59%) [97]. Although interesting, this meta-analysis was compromised by the inclusion of PPGLs with various origins and a small number of PHEOs, as well as by limiting comparisons to lesion-based analyses.

Comparisons between [⁶⁸Ga]DOTA-SSA PET/CT and [¹⁸F]FDOPA PET/CT have been performed in seven studies (five prospective, two retrospective) [63, 89, 98–102]. Separate data for PHEO could be extracted from one study [89], where [¹⁸F]FDOPA PET/CT showed better patient-based and lesion-based detection rates than did [⁶⁸Ga]DOTA-SSA PET/CT in 10 cases (100% vs. 90% and 94% vs. 81%, respectively). In the published studies involving patients with extra-adrenal PGLs, [⁶⁸Ga]DOTA-SSA PET/CT showed better patient-based and lesion-based detection rates than did [¹⁸F]FDOPA PET/CT (98% vs. 95% and 99% vs. 68%, respectively). According to a meta-analysis, [⁶⁸Ga]DOTA-SSA PET/CT detected more *SDHx*-associated PPGL lesions than did [¹⁸F]FDG PET/CT [103]. In a recent

non-comparative study from the Royal North Shore Hospital in Australia, [68Ga]DOTATATE PET/CT exhibited sensitivity of 84% (21/24) for the detection of PHEO and 100% (7/7) for the detection of PGL [104]. A higher clinical value for [68Ga]DOTA-SSA PET/CT than for [18F]FDG PET/CT was also observed in a paediatric population [102]. Among the various susceptibility genes, EPAS1 (HIF2A) and, possibly, PHD1/2 and FH remain exceptions because they cause PPGLs that concentrate a lesser amount of [68Ga]SSAs relative to the amount concentrated by SDHx-associated PPGLs [105]. The underlying mechanism for this phenotype is currently unclear. Overall, it seems that [68Ga]DOTA-SSA PET/ CT is the most sensitive tool for the detection of HNPGLs (particularly those associated with SDHD), which may be very small and/or fail to concentrate [18F]FDOPA in a sufficient amount. On the other hand, [18F]FDOPA PET/CT may be more effective than [68Ga]DOTA-SSA PET/CT in the detection of PHEOs.

[18F]FDOPA PET

Radiopharmaceutical

In many countries [¹⁸F]FDOPA is commercially available as a sterile mono- or multidose solution for intravenous use. The solution is colourless or pale yellow. In the USA, [¹⁸F]FDOPA is not approved and is used only in the setting of clinical trials.

Mechanism of cellular uptake

PPGLs can take up and decarboxylate amino acids such as dihydroxyphenylalanine (DOPA). This property depends on the activity of L-aromatic amino acid decarboxylase (AADC). DOPA, the precursor of all endogenous catecholamines, is taken up through L-type amino acid transporters (LATs), primarily LAT1. [18F]FDOPA is converted into [18F]fluorodopamine ([18F]FDA) by AADC and stored in neurosecretory vesicles.

Pharmacokinetics

After intravenous administration, [¹⁸F]FDOPA is specifically trapped by neuroendocrine tissue and follows the metabolic pathways of L-3,4-DOPA (L-DOPA). Plasma [¹⁸F]FDOPA is metabolised by catechol-O-methyltransferase (COMT) and AADC. [¹⁸F]FDOPA is quickly converted into [¹⁸F]FDA in the proximal renal tubule and other target tissues and eliminated in the urine (50% within 1 h and the rest within 12 h).

PPGLs rapidly take up [¹⁸F]FDOPA. For maximum tumour uptake, the acquisition of static clinical PET images of PPGLs using [¹⁸F]FDOPA should preferably start at 20 min after injection. After 20 min, there is a very slight decrease in



the tumour SUV, which still remains at 80% of the maximum value after 132 min [106]. Some authors use premedication with carbidopa (an AADC inhibitor) to improve the bioavailability of the tracer and decrease physiological uptake by the pancreas [107].

Synthesis and quality control

Before 2016, [¹⁸F]FDOPA was only available through electrophilic synthesis, which requires up to 4 h and exhibits low robustness, a low labelling yield (11–25% [108, 109]), and poor stability. Because it is prepared in an acid solution, electrophilically produced [¹⁸F]FDOPA needs to be neutralised using the bicarbonate buffer kit supplied by the manufacturer before administration. The pH value should range from 4.0 to 5.0.

In 2016, a nucleophilic synthesis procedure for [¹⁸F]FDOPA was validated and significantly improved the robustness of radiolabelling. This increased the radiolabelling yield and provided a ready-to-use radiopharmaceutical that remains stable for 12 h.

The two formulations seem to be equivalent, and no additional quality control is needed. Striatal uptake of [¹⁸F]FDOPA suggests the integrity of the labelled molecule and can be used as an internal control.

Drug interactions and side effects

Local pain during injection has been reported for [¹⁸F]FDOPA produced by electrophilic synthesis, probably because of the acidic pH.

Haloperidol and reserpine have been reported to increase and decrease striatal [¹⁸F]FDOPA retention, respectively [110, 111]. There is no report of drug interaction in cases involving PPGLs.

Recommended activity

2-4 Mbq/kg.

Administration

Intravenous.

Radiation dosimetry

The effective dose in adults is 0.025 mSv/MBq [67]. An additional radiation dose is delivered by CT, with the value being dependent on the scanning parameters.



Pregnancy

The use of radiopharmaceuticals is generally contraindicated in pregnancy. However, if clinically necessary, a decision to perform imaging in cases of known or suspected pregnancy should be based on an analysis of the benefits versus the possible risks to the foetus. Please refer to the section on fluorine-18 (¹⁸F)-labelled FDG PET for additional details.

Breastfeeding

Breastfeeding should be discontinued for 12 h after treatment.

Patient preparation

Patients should fast for 3–4 h, because other amino acids can competitively inhibit [¹⁸F]FDOPA influx. The administration of 200 mg of carbidopa 1 h before [¹⁸F]FDOPA injection reportedly increases the tumour uptake, although this is not recommended in the setting of PPGL [107].

Image acquisition

· Timing of imaging and image fields

Scans are generally obtained from 20 to 60 min after tracer injection, from the base of the skull to the mid-thighs or for the whole body, depending on the clinical setting.

- Optional images
- Early acquisition (10 min after tracer injection) centred over the abdomen may be obtained to overcome difficulties in localisation of abdominal PGLs located near the hepatobiliary system due to physiological tracer elimination.
- Early acquisition centred over the neck (from 10 to 20 min) may be performed in patients with MEN2 and persistent MTC [112]. MTCs often show rapid washout and are better visualised on early images [113].

Image reconstruction

Data may be acquired in the 3D or 2D mode. Iterative reconstruction algorithms represent the current standard for routine clinical practice.

Image analysis

Visual analysis

Physiological distribution Uptake can be observed in the striatum, kidneys, pancreas, liver, gallbladder, biliary tract, and

duodenum. The adrenal glands can be observed with variable uptake intensity.

Pathological uptake Any non-physiological extra-adrenal focal uptake, asymmetrical adrenal uptake that is accompanied by enlarged glands, or more intense adrenal uptake relative to the liver uptake that is accompanied by enlarged glands is considered abnormal.

Quantification

Various PET-derived quantitative indices have been found to exhibit a correlation with tumour secretion [51].

Pitfalls

False-positive findings

False-positive findings may be related to tracer uptake by other NETs as well as tumours located in the pituitary gland (e.g. prolactinomas) [114] or, rarely, other tumour types [115]. Abnormal moderate uptake may be occasionally caused by inflammatory processes.

False-negative findings

SDHx-associated PPGLs, mainly those arising from the sympathetic paraganglionic system, can be associated with falsenegative findings.

Diagnostic accuracy

A recent meta-analysis including 11 studies involving 275 patients with PPGLs showed that the pooled sensitivity and specificity in a lesion-based analysis of [18F]FDOPA PET/CT were 79% (95% CI, 76–81%) and 95% (95% CI, 84–99%), respectively [116]. The two most important factors associated with [18F]FDOPA positivity include the embryological origin (parasympathetic vs. sympathetic) of the PPGL and the SDHx mutation status of patients. One advantage of [18F]FDOPA PET/CT over [123] MIBG scintigraphy and other radiopharmaceuticals is the limited uptake by normal adrenal glands. This is very helpful in the detection of small PHEOs [101]. As mentioned earlier, [18F]FDOPA PET/CT is an excellent firstline imaging tool for HNPGLs, with sensitivity of >90% observed in various independent studies [51, 55, 59, 60, 117–120]. One contributing factor to this high sensitivity is the absence of physiological uptake in the adjacent structures. The reported patient- and lesion-based specificity of [¹⁸F]FDOPA is 94% [59, 121–125] and 100% [59, 121], respectively. The sensitivity for the detection of sporadic PHEOs is also very high (almost 100%) relative to the sensitivity for the detection of SDHB/D-associated PPGLs [51, 55,

59, 116, 117]. With regard to metastatic disease, [¹⁸F]FDOPA PET/CT was found to perform better for *SDHB*-negative PPGLs than for *SDHB*-positive PPGLs (sensitivity: 93% vs. 20%, respectively) [59, 62, 121, 122]. In contrast, recent studies found that [¹⁸F]FDOPA PET/CT shows very high sensitivity for the detection of *VHL*-, *EPAS1* (*HIF2A*)-, and *FH*-associated PPGLs, which are often multiple and recurrent and occasionally exhibit a fairly high metastatic potential [100, 105, 126].

¹⁸FIFDG PET

Radiopharmaceutical

[¹⁸F]FDG is commercially available as a ready-to-use, sterile, mono- or multidose solution for intravenous use.

Mechanism of cellular uptake

[¹⁸F]FDG is taken up by tumour cells via glucose membrane transporters and phosphorylated by hexokinase into [¹⁸F]FDG-6P. [¹⁸F]FDG-6P does not follow further enzymatic pathways and shows accumulation proportional to the cellular glycolytic rate. Interestingly, PPGLs with underlying *SDHx* mutations are more avid for [¹⁸F]FDG than are the other subtypes, mainly because of the accumulation of succinate due to Krebs cycle blockade. Succinate functions as an oncometabolite, inducing metabolic reprogramming (pseudohypoxia) [127–132] and activating the surrounding stromal tissue [133, 134]. Other PPGLs exhibit variable uptake.

Pharmacokinetics

After intravenous administration, [¹⁸F]FDG is rapidly cleared from the blood and concentrates in the brain (8%), heart wall (4%), lungs (3%), spleen (0.3%), and liver (5%). The majority is excreted unaltered by the kidneys; 20% of the injected dose is recovered in the urine within 2 h [67].

Synthesis and quality control

[¹⁸F]FDG is commercially available or prepared in-house as a ready-to-use solution in conformation with European/US pharmacopoeia.

Drug interactions and side effects

Blood glucose levels must be measured prior to the administration of [¹⁸F]FDG. Some general recommendations have been described for patients with diabetes mellitus [135]. In patients receiving chemotherapy, the PET study should be



performed after a minimum of 10 days following the last dose or as close to the next cycle as possible.

Recommended activity

2-5 MBq/kg.

Administration

Intravenous.

Radiation dosimetry

The effective dose is 0.019 mSv/MBq [67]. An additional radiation dose is delivered by CT, with the value being dependent on the scanning parameters.

Pregnancy

The use of radiopharmaceuticals is generally contraindicated in pregnancy. A decision to perform imaging in cases of known or suspected pregnancy should be based on an analysis of the benefits versus the possible risks to the foetus. The International Commission on Radiological Protection reports that the administration of 259 MBq of [18F]FDG in an adult woman results in an absorbed radiation dose of 4.7 mGy for the nongravid uterus (i.e. 0.018 mGy/MBq) [136]. Direct measurements of [18F]FDG uptake suggest somewhat higher doses than those currently described in standard models, although these doses remain reasonably low [137, 138]. A pregnancy test may help in making a decision. In the event of doubt and the absence of an emergency, the 10-day rule should be adopted. In Europe, national guidelines may apply [135].

Breastfeeding

Breastfeeding should be discontinued for 12 h after injection.

Patient preparation

Patients must fast for at least 6 h before [¹⁸F]FDG injection. Approximately 35% of patients with PHEO exhibit secondary diabetes; therefore, blood glucose should be monitored and carefully controlled before the PET study in such cases. During [¹⁸F]FDG injection and the subsequent uptake phase, patients should remain seated or recumbent in a warm, dark, and quiet room. The use of beta blockers for reducing BAT is contraindicated in the setting of PPGL, because unopposed alpha-adrenoreceptor stimulation can precipitate a hypertensive crisis.



Image acquisition

Timing of imaging

Scans are generally obtained at 60 min (45 to 90 min) after injection.

Imaging field

Imaging is performed from the base of the skull to the midthighs or for the whole body, depending on the clinical setting.

Image reconstruction

Images are acquired in the 3D or 2D mode. Iterative reconstruction algorithms represent the current standard for routine clinical practice.

Image analysis

Visual analysis

Physiological distribution The brain cortex, salivary glands, lymphatic tissue comprising Waldeyer's ring, muscles, brown fat, myocardium, mediastinum, liver, kidneys and bladder, gastrointestinal tract, testis, uterus, and ovaries (before menopause) show normal [¹⁸F]FDG uptake. Physiological [¹⁸F]FDG uptake in BAT occurs predominantly in younger patients. In patients with PHEO, BAT uptake is frequently increased because of brown adipocyte cell stimulation by norepinephrine. Physiological [¹⁸F]FDG uptake in normal adrenal glands is low, even after contralateral adrenalectomy for PHEO.

Pathological uptake Any non-physiological extra-adrenal focal uptake or more intense adrenal uptake relative to the liver uptake, accompanied by enlarged glands, is considered abnormal.

Quantification

Various quantitative indices can be described. Highly elevated uptake values are observed for *SDHx*-associated PPGLs.

Pitfalls

False-positive findings

In the absence of any hormonal secretion (so-called biochemically silent tumours), several differential diagnoses must be considered for adrenal masses with high uptake (maximum SUV ratio for the adrenal gland/liver, >2): adrenocortical carcinoma, primary lymphoma, metastasis, some cases of

myelolipoma, and oncocytoma [139]. When masses show moderate [18F]FDG uptake, the following etiologies should be considered as differential diagnoses: adrenocortical adenoma, some cases of myelolipoma, ganglioneuroma, adrenal gland metastasis (small lesions or metastasis from cancer with a lower malignant potential, sarcoma), haematoma, and adrenocortical hyperplasia.

False-negative findings

Non-FDG-avid sporadic PHEOs; non-FDG-avid retroperitoneal PGLs; MEN2-related PHEOs; and HNPGLs may be associated with false-negative findings.

Diagnostic accuracy

[¹⁸F]FDG PET positivity is a well-established feature of PPGL [55, 132, 140, 141]. Features that are suggestive of PHEO include the lack of vena cava involvement, unilateral involvement, and BAT uptake. The sensitivity is high (80–100%), while the specificity is low, as observed for any malignancy. Similar to the uptake of other PPGL-specific radiotracers, that of [¹⁸F]FDG during PET/CT is influenced by the genetic status [140–142]. Although [¹⁸F]FDG PET/CT is well accepted for MEN2-associated PHEOs, it only shows positivity in approximately 40% of patients [140]. However, it shows strong diagnostic potential for metastatic PPGLs, particularly those associated with *SDHB* mutations (sensitivity per lesion: 83% for *SDHB*-positive tumours vs. 62% for *SDHB*-negative tumours) [55, 140].

Other tracers

Technetium-99 m (99mTc)-labelled hydrazinonicotinamide-Tyr(3)-octreotide (TOC) is increasingly gaining acceptance as a new radiopharmaceutical for the diagnosis of SSTRexpressing tumours [143, 144]. In addition, [18F]FDA has been developed and is currently in use as an experimental tracer at the National Institutes of Health. It is captured by tumour cells via the NE transporter system and stored in intracellular vesicles. [18F]FDA PET/CT seems to be a very promising tool for the detection of PGLs associated with the sympathetic nervous system [53, 54, 145, 146]. Carbon-11 (11C)-labelled hydroxyephedrine (HED) has also been evaluated, but its synthesis is complex. Moreover, the short half-life of ¹¹C is a major drawback to its routine clinical use [147–151]. MIBG analogues for PET imaging have been used in a few studies, to our knowledge [152–155]. The influence of some new drugs such as histone deacetylase inhibitors on uptake of tracers is also subject to investigations [156].

SPECT versus PET imaging protocols

Both [123I]MIBG and [111In]pentetreotide scintigraphy are well-established modalities for staging and restaging as well as the follow-up of PPGLs. SPECT/CT has now become more widely available and offers the advantage of sequential acquisition of both morphological and functional data, thus increasing diagnostic confidence in terms of image interpretation and disease localisation, while enhancing sensitivity. These techniques are associated with some constraints, including prolonged imaging, relatively prolonged uptake times prior to imaging, and the presence of some gastrointestinal tract artefacts necessitating bowel cleansing, thyroid blockade, or temporary withdrawal of certain drugs that can interfere with appropriate image interpretation. The low resolution of conventional SPECT imaging can also limit the detection of small lesions. In addition, SPECT does not provide a quantitative estimate of tumour uptake, and quantitative SPECT/CT is not widely used in the clinic. Accordingly, the use of PET imaging has been increasing because of some technical as well as clinical advantages over SPECT. Currently, [18F]FDG is the most accessible tracer and plays an important role in the evaluation of these tumours, particularly SDHx-related PPGLs [55, 140]. [18F]FDOPA is also available, albeit in only a few countries. Furthermore, it is not yet approved by the Food and Drug Administration for use in the USA. Nevertheless, it is a sensitive radiotracer for the evaluation of sporadic and some metastatic PPGLs. Other tracers such as [18F]FDA and [11C]HED, which are very specific for chromaffin/ganglionic cells, are unfortunately not available at most centres and not approved by the Food and Drug Administration. Because of recent and excellent results obtained with PET imaging using various [68Ga]SSAs for patients with hereditary and non-hereditary PPGLs, [68Ga]DOTATATE is approved by the Food and Drug Administration while [68Ga]DOTATOC is approved by the EMA for the evaluation of PPGLs and GEP NETs, respectively. Both of these are now in use worldwide (Table 2).

Recommendations for clinical practice according to different clinical scenarios

Successful PPGL management requires an interdisciplinary team approach. Precise identification of the clinical context and genetic status of patients enables the personalised use of functional imaging modalities [4, 140, 157–159] (Table 3). Since the European Association of Nuclear Medicine 2012 guidelines were issued, the excellent results obtained with [⁶⁸Ga]DOTA-SSAs have simplified the imaging approach for PPGL patients [160].



Table 2 Radiopharmaceuticals used for phaeochromocytomas and paragangliomas

Tracer	Molecular target	Retention
[¹²³ I]MIBG, [¹⁸ F]FDA or [¹¹ C]HED	Norepinephrine transporter	Neurosecretory vesicles
[¹⁸ F]FDOPA	Neutral amino acid transporter system L (LATs)	Decarboxylation (AADC)
		and retention in neurosecretory vesicles as [18F]FDA
[⁶⁸ Ga]Ga-DOTATOC /DOTATATE/DOTANOC [¹⁸ F]FDG	Somatostatin receptors	Internalisation (agonists)
	Glucose transporters (GLUTs)	Phosphorylation (hexokinase)

[123 T]MIBG: iodine-123-labelled meta-iodobenzylguanidine, [18 F]FDA: fluorine-18-labelled fluorodopamine, [11 C]HED: carbon-11-labelled meta-hydroxyephedrine, [18 F]FDOPA: fluorine-18-labelled fluoro-1-dopa, [18 F]FDG: fluorine-18-labelled fluorodeoxyglucose, DOTATOC: DOTA-Tyr3-octreotide (edotreotide), DOTATATE: DOTA-Tyr3-octreotate (oxodotreotide), DOTANOC: DOTA-Nal3-octreotide, AADC: aromatic L-amino acid decarboxylase

Apparently sporadic non-metastatic PHEO

[¹²³I]MIBG scintigraphy is less sensitive than [¹⁸F]FDOPA PET/CT and superior to [¹¹¹In]pentetreotide in the localisation of non-metastatic sporadic PHEO. However, [¹²³I]MIBG scintigraphy or [¹⁸F]FDOPA PET/CT seem to be adequate for confirming the diagnosis of large sporadic PHEOs, including rarely occurring non-hypersecreting PHEOs. Compared with [¹²³I]MIBG scintigraphy, [¹⁸F]FDOPA PET/CT imaging has fewer practical constraints and no drug interactions that can limit PHEO detection, while [¹⁸F]FDG can provide genotypic information that is tightly linked to tumour behaviour (i.e., *SDHB*).

HNPGL

[¹⁸F]FDOPA and [⁶⁸Ga]DOTA-SSAs appear to be the most sensitive radiopharmaceuticals for PET imaging in sporadic cases. In patients with *SDHx*-associated tumours, [⁶⁸Ga]DOTA-SSA PET/CT can detect very small lesions that can be overlooked by [¹⁸F]FDOPA PET/CT. If [¹⁸F]FDOPA or

[⁶⁸Ga]DOTA-SSA PET/CT is not available, SSTR scintigraphy may be used as an alternative, considering the limitations associated with the spatial resolution of SPECT. [¹⁸F]FDG PET exhibits high sensitivity in the setting of *SDHx*-related HNPGLs and can complement [¹⁸F]FDOPA PET/CT for the detection of additional thoracic/abdominal PGLs.

Retroperitoneal, extra-adrenal, non-metastatic PGLs

In cases involving retroperitoneal, extra-adrenal, non-renal masses, imaging should enable the differentiation of PGLs from neurogenic tumours, lymph node diseases, and mesenchymal tumours. Therefore, the specificity of functional imaging provides an important contribution. Once the diagnosis of PGL has been established, the multiplicity of extra-adrenal localisations should be considered. In this context, ¹⁸F-FDOPA and [⁶⁸Ga]DOTA-SSAs are more specific than [¹⁸F]FDG and can identify more lesions. Therefore, [⁶⁸Ga]DOTA-SSA PET/CT is probably the preferred imaging modality at present, particularly for patients with *SDHx* mutations.

Table 3 Proposed clinical algorithm for nuclear imaging investigations in cases of phaeochromocytomas and paragangliomas

	First choice	Second choice	Third choice (if [¹⁸ F]FDOPA or [⁶⁸ Ga]Ga-SSA is not available)
PHEO (sporadic)	[¹⁸ F]FDOPA or [¹²³ I]MIBG	[⁶⁸ Ga]SSA	[¹⁸ F]FDG
Inherited PHEO (except <i>SDHx</i>): NF1/RET/VHL/MAX	[¹⁸ F]FDOPA	[¹²³ I]MIBG or [⁶⁸ Ga]SSA	[¹⁸ F]FDG
HNPGL (sporadic)	[⁶⁸ Ga]SSA	[¹⁸ F]FDOPA	[¹¹¹ In]SSA/[^{99m} Tc]SSA
Extra-adrenal sympathetic and/or multifocal and/or metastatic and/or <i>SDHx</i> mutation	[⁶⁸ Ga]SSA	[¹⁸ F]FDG and [¹⁸ F]FDOPA	[¹⁸ F]FDG and [¹²³ I]MIBG or [¹⁸ F]FDG and [¹¹¹ In]SSA/[^{99m} Tc]SSA

The above algorithm can be proposed as per the clinical situation. This algorithm should be practically adapted in each institution and evolve with time. PHEO: phaeochromocytoma, [123 I]MIBG: iodine-123-labelled meta-iodobenzylguanidine, [18 F]FDA: fluorine-18-labelled fluorodopamine, [18 F]FDOPA: fluorine-18-labelled fluorodihydroxyphenylalanine, [18 F]FDG: fluorine-18-labelled fluorodeoxyglucose, [68 Ga]SSA: gallium-68-labelled somatostatin analogue, [111 In]SSA: indium-111-labelled somatostatin analogue, [99m Tc]SSA: technetium-99-labelled somatostatin analogue, NF1/RET/VHL/MAX: neurofibromin 1/rearranged during transfection proto-oncogene/von Hippel–Lindau/myc-associated factor X, HNPGL: head and neck paraganglioma, SDHx: succinate dehydrogenase subunits.



Metastatic PPGLs

[18F]FDOPA shows very good results in terms of the detection of metastatic lesions in patients with sporadic PPGLs. However, its sensitivity decreases in the presence of SDHx mutations. [68Ga]DOTA-SSA has shown better results compared with those of [18F]FDOPA, regardless of the genetic background; therefore, it is becoming the imaging modality of choice for metastatic PPGLs. It can also be used to determine whether a patient is likely to benefit from PRRT. [18F1FDOPA PET/CT can be used as a second-line imaging modality when SDHB mutations are absent or the genetic status is unknown, whereas [18F]FDG PET/CT can be considered for SDHB-associated metastatic PPGLs. [123I]MIBG may lead to significant underestimation of metastatic disease and result in inappropriate management. [123I]MIBG and [18F]FDOPA images do not completely overlap. Furthermore, [123I]MIBG is a theranostic radiopharmaceutical, and [123I]MIBG imaging can be used to determine whether a patient is eligible for [131]MIBG therapy. The clinical benefits of using high-specific-activity [I¹³¹]MIBG (Azedra®) for patients with metastatic, recurrent, and/or unresectable PPGLs will promote the use of MIBG imaging for in vivo detection of the cell membrane NE transporter system. Azedra® was recently approved by the Food and Drug Administration. Although not widely available, the PET-equivalent [124]]MIBG offers significant advantages in terms of the spatial resolution and its ability to quantify uptake for dosimetry calculations.

VHL- and RET (MEN2)-associated PPGLs

Currently, there are limited data with respect to imaging studies for patients with VHL and RET mutations. Nevertheless, there are two advantages that circumvent this problem. First, as mentioned above, MEN2 PHEOs always exhibit an adrenergic biochemical phenotype; therefore, the tumours are located exclusively in the adrenal glands. As a result, positive biochemistry and CT/MRI images showing a tumour in the adrenal glands can collectively confirm the presence of PHEOs. In this scenario, functional imaging is not needed. Exceptions include extra-adrenal tumours or PHEOs measuring >5 cm, which are likely to become metastatic. However, such cases are rare. Second, these tumours, as well as those related to VHL mutations, are rarely metastatic (<5%). Thus, whole-body imaging is necessary only if a lesion cannot be found in the adrenal glands. [18F]FDG PET and [18F]FDOPA PET/CT together with MRI can help in preoperative mapping of PHEOs within both adrenal glands and guide surgeons toward the most appropriate (feasible) approach.

Screening for carriers of SDHx mutations

The penetrance of disease varies across PPGL syndromes. Although *SDHD* and *SDHB* mutations both cause autosomal dominant diseases, the disease penetrance is different. The penetrance of *SDHD*-related PPGL is modulated by maternal imprinting. In other words, the disease almost always occurs only when the mutations are inherited from the father. Paternally inherited *SDHD* mutations are associated with a very high overall disease penetrance (>80%), whereas *SDHB* mutations are associated with an estimated penetrance of only 20–40% [161–164]. A lower *SDHD*-related disease penetrance may be observed in studies including less severe mutations [165].

The optimal follow-up algorithm for non-proband SDHx-associated PPGLs has not yet been validated, although it most likely requires more frequent and complete imaging studies than does the algorithm for sporadic PPGLs. The aim is to detect tumours in the early stages of development in order to minimise tumour spread and new cranial nerve impairment related to SDHD mutations [166], facilitate curative treatment, and potentially reduce the occurrence of metastases, particularly in patients with more aggressive genotypes. During initial staging, [18F]FDG PET should provide adequate sensitivity and specificity for whole-body imaging, with limited radiation exposure (2-2.5 mSv for the radiopharmaceutical, 1-3 mSv for CT) and very low, if any, risks [167]. On the basis of clinical studies performed in patients with PPGLs, [68Ga]DOTA-SSA PET should be prioritised, if available, over [18F]FDG PET, although its indication in the setting of non-proband SDHx-associated tumours has not been specifically studied. In the absence of PPGLs, follow-up studies should include annual biochemical screening and MRI at regular intervals [168].

Acknowledgements We thank the EANM Committees, EANM National Societies, and the SNMMI bodies for their review and contribution.

K.P. was supported by the Intramural Research Program of NIH, NICHD.

Compliance with Ethical Standards

Conflict of interest RH has received research funding from Ipsen, Novartis, and Clarity Pharmaceuticals and holds stock in Telix Pharmaceuticals on behalf of his institution.

NPT has received consultant/advisory board/honoraria (current/past) from Y-mAbs, Progenics, Bayer, and MedImmune/AstraZeneca and sponsored trials/research support from ImaginAb, Genentech, and Actinium Pharma/FluoroPharma.

The other authors declare that they have no conflict of interest.

Ethical approval This article does not contain any studies with human participants performed by any of the authors.



References

- Lenders JW, Duh QY, Eisenhofer G, Gimenez-Roqueplo AP, Grebe SK, Murad MH, et al. Pheochromocytoma and paraganglioma: an endocrine society clinical practice guideline. J Clin Endocrinol Metab. 2014;99:1915–42.
- Lloyd RV, Osamura RY, Kloppel G, Rosai JWHO. Classification of Tumours of Endocrine Organs. Lyon: IARC Press; 2017.
- Fassnacht M, Arlt W, Bancos I, Dralle H, Newell-Price J, Sahdev A, et al. Management of adrenal incidentalomas: European Society of Endocrinology Clinical Practice Guideline in collaboration with the European Network for the Study of Adrenal Tumours. Eur J Endocrinol. 2016;175:G1–G34.
- Crona J, Taieb D, Pacak K. New Perspectives on Pheochromocytoma and Paraganglioma: Toward a Molecular Classification. Endocr Rev. 2017;38:489–515.
- Jafri M, Whitworth J, Rattenberry E, Vialard L, Kilby G, Kumar AV, et al. Evaluation of SDHB, SDHD and VHL gene susceptibility testing in the assessment of individuals with non-syndromic phaeochromocytoma, paraganglioma and head and neck paraganglioma. Clin Endocrinol. 2013;78:898–906.
- Neumann HP, Erlic Z, Boedeker CC, Rybicki LA, Robledo M, Hermsen M, et al. Clinical predictors for germline mutations in head and neck paraganglioma patients: cost reduction strategy in genetic diagnostic process as fall-out. Cancer Res. 2009;69:3650– 6
- Papathomas TG, Gaal J, Corssmit EP, Oudijk L, Korpershoek E, Heimdal K, et al. Non-pheochromocytoma (PCC)/paraganglioma (PGL) tumours in patients with succinate dehydrogenase-related PCC-PGL syndromes: a clinicopathological and molecular analysis. Eur J Endocrinol. 2014;170:1–12.
- Pasini B, McWhinney SR, Bei T, Matyakhina L, Stergiopoulos S, Muchow M, et al. Clinical and molecular genetics of patients with the Carney-Stratakis syndrome and germline mutations of the genes coding for the succinate dehydrogenase subunits SDHB, SDHC, and SDHD. Eur J Hum Genet. 2008;16:79–88.
- Casey RT, Warren AY, Martin JE, Challis BG, Rattenberry E, Whitworth J, et al. Clinical and Molecular Features of Renal and Pheochromocytoma/Paraganglioma Tumour Association Syndrome (RAPTAS): Case Series and Literature Review. J Clin Endocrinol Metab. 2017;102:4013–22.
- Eisenhofer G, Pacak K, Huynh TT, Qin N, Bratslavsky G, Linehan WM, et al. Catecholamine metabolomic and secretory phenotypes in phaeochromocytoma. Endocr Relat Cancer. 2011;18:97–111.
- Hannah-Shmouni F, Pacak K, Stratakis CA. Metanephrines for Evaluating Palpitations and Flushing. JAMA. 2017;318:385–6.
- Eisenhofer G, Goldstein DS, Walther MM, Friberg P, Lenders JW, Keiser HR, et al. Biochemical diagnosis of pheochromocytoma: how to distinguish true- from false-positive test results. J Clin Endocrinol Metab. 2003;88:2656–66.
- Leung K, Stamm M, Raja A, Low G. Pheochromocytoma: the range of appearances on ultrasound, CT, MRI, and functional imaging. AJR Am J Roentgenol. 2013;200:370–8.
- Canu L, Van Hemert JAW, Kerstens MN, Hartman RP, Khanna A, Kraljevic I, et al. CT Characteristics of Pheochromocytoma: Relevance for the Evaluation of Adrenal Incidentaloma. J Clin Endocrinol Metab. 2019;104:312–8.
- Turkova H, Prodanov T, Maly M, Martucci V, Adams K, Widimsky J, Jr., et al. Characteristics and outcomes of metastatic SDHB and sporadic pheochromocytoma/paraganglioma: An National Institutes of Health Study. 2016;22:302–14.
- 16. Hescot S, Curras-Freixes M, Deutschbein T, van Berkel A, Vezzosi D, Amar L, et al. European Network for the Study of Adrenal Tumours (ENS@T). Prognosis of Malignant Pheochromocytoma and Paraganglioma (MAPP-Prono Study):

- A European Network for the Study of Adrenal Tumours Retrospective Study. J Clin Endocrinol Metab. 2019;104:2367–74
- Crona J, Lamarca A, Ghosal S, Welin S, Skogseid B, Pacak K. Genotype-phenotype correlations in pheochromocytoma and paraganglioma. Endocr Relat Cancer. 2019. https://doi.org/10. 1530/ERC-19-0024.
- Fishbein L, Khare S, Wubbenhorst B, DeSloover D, D'Andrea K, Merrill S, et al. Whole-exome sequencing identifies somatic ATRX mutations in pheochromocytomas and paragangliomas. Nat Commun. 2015;6:6140.
- Zelinka T, Musil Z, Duskova J, Burton D, Merino MJ, Milosevic D, et al. Metastatic pheochromocytoma: does the size and age matter? Eur J Clin Investig. 2011;41:1121–8.
- Eisenhofer G, Lenders JW, Siegert G, Bornstein SR, Friberg P, Milosevic D, et al. Plasma methoxytyramine: a novel biomarker of metastatic pheochromocytoma and paraganglioma in relation to established risk factors of tumour size, location and SDHB mutation status. Eur J Cancer. 2012;48:1739–49.
- Kong G, Schenberg T, Yates CJ, Trainer A, Sachithanandan N, Iravani A, et al. The role of 68Ga-DOTA-Octreotate (GaTate) PET/CT in follow-up of SDH-associated pheochromocytoma and paraganglioma (PPGL). J Clin Endocrinol Metab. 2019. https://doi.org/10.1210/jc.2019-00018.
- Heimburger C, Veillon F, Taieb D, Goichot B, Riehm S, Petit-Thomas J, et al. Head-to-head comparison between 18F-FDOPA PET/CT and MR/CT angiography in clinically recurrent head and neck paragangliomas. Eur J Nucl Med Mol Imaging. 2017;44: 979–87
- Kong G, Grozinsky-Glasberg S, Hofman MS, Callahan J, Meirovitz A, Maimon O, et al. Efficacy of Peptide Receptor Radionuclide Therapy for Functional Metastatic Paraganglioma and Pheochromocytoma. J Clin Endocrinol Metab. 2017;102: 3278–87.
- Rutgers M, Tytgat GA, Verwijs-Janssen M, Buitenhuis C, Voute PA, Smets LA. Uptake of the neuron-blocking agent metaiodobenzylguanidine and serotonin by human platelets and neuro-adrenergic tumour cells. Int J Cancer. 1993;54:290–5.
- Jaques S Jr, Tobes MC, Sisson JC. Sodium dependency of uptake of norepinephrine and m-iodobenzylguanidine into cultured human pheochromocytoma cells: evidence for uptake-one. Cancer Res. 1987;47:3920–8.
- Bomanji J, Levison DA, Flatman WD, Horne T, Bouloux PM, Ross G, et al. Uptake of iodine-123 MIBG by pheochromocytomas, paragangliomas, and neuroblastomas: a histopathological comparison. J Nucl Med. 1987;28:973–8.
- ICRP. Radiation Dose to Patients from Radiopharmaceuticals.
 ICRP Publication 53. Ann IRCP. 1988;18.
- Sinclair AJ, Bomanji J, Harris P, Ross G, Besser GM, Britton KE. Pre- and post-treatment distribution pattern of 123I-MIBG in patients with phaeochromocytomas and paragangliomas. Nucl Med Commun. 1989;10:567–76.
- Solanki KK, Bomanji J, Moyes J, Mather SJ, Trainer PJ, Britton KE. A pharmacological guide to medicines which interfere with the biodistribution of radiolabelled meta-iodobenzylguanidine (MIBG). Nucl Med Commun. 1992;13:513–21.
- Jacobson AF, Travin MI. Impact of medications on mIBG uptake, with specific attention to the heart: Comprehensive review of the literature. J Nucl Cardiol. 2015;22:980–93.
- Jacobson AF, White S, Travin MI, Tseng C. Impact of concomitant medication use on myocardial 123I-mIBG imaging results in patients with heart failure. Nucl Med Commun. 2017;38:141–8.
- Bombardieri E, Giammarile F, Aktolun C, Baum RP, Bischof Delaloye A, Maffioli L, et al. 131I/123I-metaiodobenzylguanidine (mIBG) scintigraphy: procedure guidelines for tumour imaging. Eur J Nucl Med Mol Imaging. 2010;37:2436–46.



- Bombardieri E, Aktolun C, Baum RP, Bishof-Delaloye A, Buscombe J, Chatal JF, et al. 131I/123I-metaiodobenzylguanidine (MIBG) scintigraphy: procedure guidelines for tumour imaging. Eur J Nucl Med Mol Imaging. 2003;30:BP132–9.
- Bar-Sever Z, Biassoni L, Shulkin B, Kong G, Hofman MS, Lopci E, et al. Guidelines on nuclear medicine imaging in neuroblastoma. Eur J Nucl Med Mol Imaging. 2018.
- Khafagi FA, Shapiro B, Fig LM, Mallette S, Sisson JC. Labetalol reduces iodine-131 MIBG uptake by pheochromocytoma and normal tissues. J Nucl Med. 1989;30:481–9.
- Apeldoom L, Voerman HJ, Hoefnagel CA. Interference of MIBG uptake by medication: a case report. Neth J Med. 1995;46:239

 –43.
- Estorch M, Carrio I, Mena E, Flotats A, Camacho V, Fuertes J, et al. Challenging the neuronal MIBG uptake by pharmacological intervention: effect of a single dose of oral amitriptyline on regional cardiac MIBG uptake. Eur J Nucl Med Mol Imaging. 2004;31: 1575–80.
- Zaplatnikov K, Menzel C, Dobert N, Hamscho N, Kranert WT, Gotthard M, et al. Case report: drug interference with MIBG uptake in a patient with metastatic paraganglioma. Br J Radiol. 2004;77:525–7.
- Blake GM, Lewington VJ, Fleming JS, Zivanovic MA, Ackery DM. Modification by nifedipine of 1311-metaiodobenzylguanidine kinetics in malignant phaeochromocytoma. Eur J Nucl Med. 1988;14:345-8.
- 40. Taniguchi K, Ishizu K, Torizuka T, Hasegawa S, Okawada T, Ozawa T, et al. Metastases of predominantly dopamine-secreting phaeochromocytoma that did not accumulate metaiodobenzylguanidine: imaging with whole body positron emission tomography using 18F-labelled deoxyglucose. Eur J Surg. 2001;167:866–70.
- Van Der Horst-Schrivers AN, Osinga TE, Kema IP, Van Der Laan BF, Dullaart RP. Dopamine excess in patients with head and neck paragangliomas. Anticancer Res. 2010;30:5153–8.
- van Gelder T, Verhoeven GT, de Jong P, Oei HY, Krenning EP, Vuzevski VD, et al. Dopamine-producing paraganglioma not visualized by iodine-123-MIBG scintigraphy. J Nucl Med. 1995;36: 620–2.
- Hall FT, Perez-Ordonez B, Mackenzie RG, Gilbert RW. Does Catecholamine Secretion from Head and Neck Paragangliomas Respond to Radiotherapy? Case Report and Literature Review. Skull Base. 2003;13:229–34.
- Ishibashi N, Abe K, Furuhashi S, Fukushima S, Yoshinobu T, Takahashi M, et al. Adverse allergic reaction to 131I MIBG. Ann Nucl Med. 2009;23:697–9.
- ICRP. Radiation dose to patients from radiopharmaceuticals.
 Addendum 2 to ICRP Publication 53. Ann IRCP. 1998;28:1–126.
- Tobes MC, Fig LM, Carey J, Geatti O, Sisson JC, Shapiro B. Alterations of iodine-131 MIBG biodistribution in an anephric patient: comparison to normal and impaired renal function. J Nucl Med. 1989;30:1476–82.
- Friedman NC, Hassan A, Grady E, Matsuoka DT, Jacobson AF. Efficacy of thyroid blockade on thyroid radioiodine uptake in 123I-mIBG imaging. J Nucl Med. 2014;55:211–5.
- Beauregard JM, Hofman MS, Pereira JM, Eu P, Hicks RJ. Quantitative (177)Lu SPECT (QSPECT) imaging using a commercially available SPECT/CT system. Cancer Imaging. 2011;11: 56–66
- Tran-Gia J, Lassmann M. Characterization of Noise and Resolution for Quantitative (177)Lu SPECT/CT with xSPECT Quant. J Nucl Med. 2019;60:50–9.
- Bailey DL, Willowson KP. Quantitative SPECT/CT: SPECT joins PET as a quantitative imaging modality. Eur J Nucl Med Mol Imaging. 2014;41(Suppl 1):S17–25.
- Fiebrich HB, Brouwers AH, Kerstens MN, Pijl ME, Kema IP, de Jong JR, et al. 6-[F-18]Fluoro-L-dihydroxyphenylalanine positron

- emission tomography is superior to conventional imaging with (123)I-metaiodobenzylguanidine scintigraphy, computer tomography, and magnetic resonance imaging in localizing tumours causing catecholamine excess. J Clin Endocrinol Metab. 2009;94:3922–30.
- 52. Fonte JS, Robles JF, Chen CC, Reynolds J, Whatley M, Ling A, et al. False-negative (1)(2)(3)I-MIBG SPECT is most commonly found in SDHB-related pheochromocytoma or paraganglioma with high frequency to develop metastatic disease. Endocr Relat Cancer. 2012;19:83–93.
- Ilias I, Chen CC, Carrasquillo JA, Whatley M, Ling A, Lazurova I, et al. Comparison of 6-18F-fluorodopamine PET with 123Imetaiodobenzylguanidine and 111in-pentetreotide scintigraphy in localization of nonmetastatic and metastatic pheochromocytoma. J Nucl Med. 2008;49:1613–9.
- 54. Timmers HJ, Eisenhofer G, Carrasquillo JA, Chen CC, Whatley M, Ling A, et al. Use of 6-[18F]-fluorodopamine positron emission tomography (PET) as first-line investigation for the diagnosis and localization of non-metastatic and metastatic phaeochromocytoma (PHEO). Clin Endocrinol. 2009;71:11–7.
- 55. Timmers HJ, Chen CC, Carrasquillo JA, Whatley M, Ling A, Havekes B, et al. Comparison of 18F-fluoro-L-DOPA, 18F-fluoro-deoxyglucose, and 18F-fluorodopamine PET and 123I-MIBG scintigraphy in the localization of pheochromocytoma and paraganglioma. J Clin Endocrinol Metab. 2009;94:4757–67.
- Eisenhofer G, Rivers G, Rosas AL, Quezado Z, Manger WM, Pacak K. Adverse drug reactions in patients with phaeochromocytoma: incidence, prevention and management. Drug Saf. 2007;30:1031–62.
- Hoegerle S, Altehoefer C, Ghanem N, Koehler G, Waller CF, Scheruebl H, et al. Whole-body 18F dopa PET for detection of gastrointestinal carcinoid tumours. Radiology. 2001;220:373–80.
- Kaji P, Carrasquillo JA, Linehan WM, Chen CC, Eisenhofer G, Pinto PA, et al. The role of 6-[18F]fluorodopamine positron emission tomography in the localization of adrenal pheochromocytoma associated with von Hippel-Lindau syndrome. Eur J Endocrinol. 2007;156:483–7.
- Fottner C, Helisch A, Anlauf M, Rossmann H, Musholt TJ, Kreft A, et al. 6-18F-fluoro-L-dihydroxyphenylalanine positron emission tomography is superior to 123I-metaiodobenzyl-guanidine scintigraphy in the detection of extraadrenal and hereditary pheochromocytomas and paragangliomas: correlation with vesicular monoamine transporter expression. J Clin Endocrinol Metab. 2010;95:2800–10.
- 60. King KS, Chen CC, Alexopoulos DK, Whatley MA, Reynolds JC, Patronas N, et al. Functional imaging of SDHx-related head and neck paragangliomas: comparison of 18F-fluorodihydroxyphenylalanine, 18F-fluorodopamine, 18F-fluoro-2-deoxy-D-glucose PET, 123I-metaiodobenzylguanidine scintigraphy, and 111In-pentetreotide scintigraphy. J Clin Endocrinol Metab. 2011;96:2779–85.
- Rufini V, Treglia G, Castaldi P, Perotti G, Calcagni ML, Corsello SM, et al. Comparison of 123I-MIBG SPECT-CT and 18F-DOPA PET-CT in the evaluation of patients with known or suspected recurrent paraganglioma. Nucl Med Commun. 2011;32:575–82.
- 62. Taieb D, Tessonnier L, Sebag F, Niccoli-Sire P, Morange I, Colavolpe C, et al. The role of 18F-FDOPA and 18F-FDG-PET in the management of malignant and multifocal phaeochromocytomas. Clin Endocrinol. 2008;69:580-6.
- Janssen I, Chen CC, Taieb D, Patronas NJ, Millo CM, Adams KT, et al. 68Ga-DOTATATE PET/CT in the Localization of Head and Neck Paragangliomas Compared with Other Functional Imaging Modalities and CT/MRI. J Nucl Med. 2016;57:186–91.
- 64. Krenning EP, Bakker WH, Kooij PP, Breeman WA, Oei HY, de Jong M, et al. Somatostatin receptor scintigraphy with indium-111-DTPA-D-Phe-1-octreotide in man: metabolism, dosimetry



- and comparison with iodine-123-Tyr-3-octreotide. J Nucl Med. 1992;33:652–8.
- Bombardieri E, Ambrosini V, Aktolun C, Baum RP, Bishof-Delaloye A, Del Vecchio S, et al. 111In-pentetreotide scintigraphy: procedure guidelines for tumour imaging. Eur J Nucl Med Mol Imaging. 2010;37:1441–8.
- Balon HR, Brown TL, Goldsmith SJ, Silberstein EB, Krenning EP, Lang O, et al. The SNM practice guideline for somatostatin receptor scintigraphy 2.0. J Nucl Med Technol. 2011;39:317–24.
- ICRP. Radiation Dose to Patients fromRadiopharmaceuticals: A Compendium of Current Information Related to Frequently Used Substances. ICRP Publication 128. Ann IRCP. 2015:44.
- Balon HR. Updated practice guideline for somatostatin receptor scintigraphy. J Nucl Med. 2011;52:1838.
- Bustillo A, Telischi F, Weed D, Civantos F, Angeli S, Serafini A, et al. Octreotide scintigraphy in the head and neck. Laryngoscope. 2004;114:434–40.
- Duet M, Sauvaget E, Petelle B, Rizzo N, Guichard JP, Wassef M, et al. Clinical impact of somatostatin receptor scintigraphy in the management of paragangliomas of the head and neck. J Nucl Med. 2003;44:1767–74.
- Koopmans KP, Jager PL, Kema IP, Kerstens MN, Albers F, Dullaart RP. 111In-octreotide is superior to 123Imetaiodobenzylguanidine for scintigraphic detection of head and neck paragangliomas. J Nucl Med. 2008;49:1232–7.
- Muros MA, Llamas-Elvira JM, Rodriguez A, Ramirez A, Gomez M, Arraez MA, et al. 111In-pentetreotide scintigraphy is superior to 123I-MIBG scintigraphy in the diagnosis and location of chemodectoma. Nucl Med Commun. 1998;19:735–42.
- Schmidt M, Fischer E, Dietlein M, Michel O, Weber K, Moka D, et al. Clinical value of somatostatin receptor imaging in patients with suspected head and neck paragangliomas. Eur J Nucl Med Mol Imaging. 2002;29:1571–80.
- Telischi FF, Bustillo A, Whiteman ML, Serafini AN, Reisberg MJ, Gomez-Marin O, et al. Octreotide scintigraphy for the detection of paragangliomas. Otolaryngol Head Neck Surg. 2000;122:358–62.
- Gimenez-Roqueplo AP, Caumont-Prim A, Houzard C, Hignette C, Hernigou A, Halimi P, et al. Imaging work-up for screening of paraganglioma and pheochromocytoma in SDHx mutation carriers: a multicenter prospective study from the PGL.EVA Investigators. J Clin Endocrinol Metab. 2013;98:E162–73.
- Kaltsas GA, Mukherjee JJ, Grossman AB. The value of radiolabelled MIBG and octreotide in the diagnosis and management of neuroendocrine tumours. Ann Oncol. 2001;12(Suppl 2): S47–50.
- van der Harst E, de Herder WW, Bruining HA, Bonjer HJ, de Krijger RR, Lamberts SW, et al. [(123)I]metaiodobenzylguanidine and [(111)In]octreotide uptake in benign and malignant pheochromocytomas. J Clin Endocrinol Metab. 2001;86:685–93.
- Tenenbaum F, Lumbroso J, Schlumberger M, Mure A, Plouin PF, Caillou B, et al. Comparison of radiolabeled octreotide and metaiodobenzylguanidine (MIBG) scintigraphy in malignant pheochromocytoma. J Nucl Med. 1995;36:1–6.
- Wild D, Macke HR, Waser B, Reubi JC, Ginj M, Rasch H, et al. 68Ga-DOTANOC: a first compound for PET imaging with high affinity for somatostatin receptor subtypes 2 and 5. Eur J Nucl Med Mol Imaging. 2005;32:724.
- Wild D, Schmitt JS, Ginj M, Macke HR, Bernard BF, Krenning E, et al. DOTA-NOC, a high-affinity ligand of somatostatin receptor subtypes 2, 3 and 5 for labelling with various radiometals. Eur J Nucl Med Mol Imaging. 2003;30:1338–47.
- Reubi JC, Schar JC, Waser B, Wenger S, Heppeler A, Schmitt JS, et al. Affinity profiles for human somatostatin receptor subtypes SST1-SST5 of somatostatin radiotracers selected for scintigraphic and radiotherapeutic use. Eur J Nucl Med. 2000;27:273–82.

- 82. Fani M, Nicolas GP, Wild D. Somatostatin Receptor Antagonists for Imaging and Therapy. J Nucl Med. 2017;58:61S–6S.
- Pettinato C, Sarnelli A, Di Donna M, Civollani S, Nanni C, Montini G, et al. 68Ga-DOTANOC: biodistribution and dosimetry in patients affected by neuroendocrine tumours. Eur J Nucl Med Mol Imaging. 2008;35:72–9.
- 84. Cherk MH, Kong G, Hicks RJ, Hofman MS. Changes in biodistribution on (68)Ga-DOTA-Octreotate PET/CT after long acting somatostatin analogue therapy in neuroendocrine tumour patients may result in pseudoprogression. Cancer Imaging. 2018;18:3.
- Sandstrom M, Velikyan I, Garske-Roman U, Sorensen J, Eriksson B, Granberg D, et al. Comparative biodistribution and radiation dosimetry of 68Ga-DOTATOC and 68Ga-DOTATATE in patients with neuroendocrine tumours. J Nucl Med. 2013;54:1755–9.
- Aalbersberg EA, de Wit-van der Veen BJ, Versleijen MWJ, Saveur LJ, Valk GD, Tesselaar MET, et al. Influence of lanreotide on uptake of (68)Ga-DOTATATE in patients with neuroendocrine tumours: a prospective intra-patient evaluation. Eur J Nucl Med Mol Imaging. 2019;46:696–703.
- Lasnon C, Hicks RJ, Beauregard JM, Milner A, Paciencia M, Guizard AV, et al. Impact of point spread function reconstruction on thoracic lymph node staging with 18F-FDG PET/CT in nonsmall cell lung cancer. Clin Nucl Med. 2012;37:971–6.
- Castellucci P, Pou Ucha J, Fuccio C, Rubello D, Ambrosini V, Montini GC, et al. Incidence of increased 68Ga-DOTANOC uptake in the pancreatic head in a large series of extrapancreatic NET patients studied with sequential PET/CT. J Nucl Med. 2011;52: 886–90.
- 89. Archier A, Varoquaux A, Garrigue P, Montava M, Guerin C, Gabriel S, et al. Prospective comparison of (68)Ga-DOTATATE and (18)F-FDOPA PET/CT in patients with various pheochromocytomas and paragangliomas with emphasis on sporadic cases. Eur J Nucl Med Mol Imaging. 2016;43:1248–57.
- Hofman MS, Lau WF, Hicks RJ. Somatostatin receptor imaging with 68Ga DOTATATE PET/CT: clinical utility, normal patterns, pearls, and pitfalls in interpretation. Radiographics. 2015;35:500– 16
- Naji M, Al-Nahhas A. (68)Ga-labelled peptides in the management of neuroectodermal tumours. Eur J Nucl Med Mol Imaging. 2012;39(Suppl 1):S61–7.
- Naji M, Zhao C, Welsh SJ, Meades R, Win Z, Ferrarese A, et al. 68Ga-DOTA-TATE PET vs. 123I-MIBG in identifying malignant neural crest tumours. Mol Imaging Biol. 2011;13:769–75.
- Sharma P, Thakar A, Suman Kc S, Dhull VS, Singh H, Naswa N, et al. 68Ga-DOTANOC PET/CT for Baseline Evaluation of Patients with Head and Neck Paraganglioma. J Nucl Med. 2013;54:841–7.
- Kroiss A, Shulkin BL, Uprimny C, Frech A, Gasser RW, Url C, et al. (68)Ga-DOTATOC PET/CT provides accurate tumour extent in patients with extraadrenal paraganglioma compared to (123)I-MIBG SPECT/CT. Eur J Nucl Med Mol Imaging. 2015;42:33–41.
- Sharma P, Mukherjee A, Karunanithi S, Naswa N, Kumar R, Ammini AC, et al. Accuracy of 68Ga DOTANOC PET/CT Imaging in Patients With Multiple Endocrine Neoplasia Syndromes. Clin Nucl Med. 2015;40:e351–6.
- Chang CA, Pattison DA, Tothill RW, Kong G, Akhurst TJ, Hicks RJ, et al. (68)Ga-DOTATATE and (18)F-FDG PET/CT in Paraganglioma and Pheochromocytoma: utility, patterns and heterogeneity. Cancer Imaging. 2016;16:22.
- Han S, Suh CH, Woo S, Kim YJ, Lee JJ. Performance of (68)Ga-DOTA-Conjugated Somatostatin Receptor Targeting Peptide PET in Detection of Pheochromocytoma and Paraganglioma: A Systematic Review and Meta-Analysis. J Nucl Med. 2019;60: 369–76.



- Kroiss A, Putzer D, Frech A, Decristoforo C, Uprimny C, Gasser RW, et al. A retrospective comparison between 68Ga-DOTA-TOC PET/CT and 18F-DOPA PET/CT in patients with extra-adrenal paraganglioma. Eur J Nucl Med Mol Imaging. 2013;40:1800–8.
- Janssen I, Blanchet EM, Adams K, Chen CC, Millo CM, Herscovitch P, et al. Superiority of [68Ga]-DOTATATE PET/CT to Other Functional Imaging Modalities in the Localization of SDHB-Associated Metastatic Pheochromocytoma and Paraganglioma. Clin Cancer Res. 2015;21:3888–95.
- Janssen I, Chen CC, Zhuang Z, Millo CM, Wolf KI, Ling A, et al. Functional Imaging Signature of Patients Presenting with Polycythemia/Paraganglioma Syndromes. J Nucl Med. 2017;58: 1236–42.
- Taieb D, Jha A, Guerin C, Pang Y, Adams KT, Chen CC, et al. 18F-FDOPA PET/CT imaging of MAX-Related Pheochromocytoma. J Clin Endocrinol Metab. 2018;103:1574– 82.
- 102. Jha A, Ling A, Millo C, Gupta G, Viana B, Lin FI, et al. Superiority of (68)Ga-DOTATATE over (18)F-FDG and anatomic imaging in the detection of succinate dehydrogenase mutation (SDHx)-related pheochromocytoma and paraganglioma in the pediatric population. Eur J Nucl Med Mol Imaging. 2018;45: 787–97
- 103. Kan Y, Zhang S, Wang W, Liu J, Yang J, Wang Z. (68)Ga-somatostatin receptor analogs and (18)F-FDG PET/CT in the localization of metastatic pheochromocytomas and paragangliomas with germline mutations: a meta-analysis. Acta Radiol. 2018;59: 1466-74
- Gild ML, Naik N, Hoang J, Hsiao E, McGrath RT, Sywak M, et al. Role of DOTATATE-PET/CT in preoperative assessment of phaeochromocytoma and paragangliomas. Clin Endocrinol. 2018. https://doi.org/10.1111/cen.13737.
- Darr R, Nambuba J, Del Rivero J, Janssen I, Merino M, Todorovic M, et al. Novel insights into the polycythemia-paragangliomasomatostatinoma syndrome. Endocr Relat Cancer. 2016;23:899– 908.
- 106. Hentschel M, Rottenburger C, Boedeker CC, Neumann HP, Brink I. Is there an optimal scan time for 6-[F-18]fluoro-L-DOPA PET in pheochromocytomas and paragangliomas? Clin Nucl Med. 2012;37:e24–9.
- 107. Timmers HJ, Hadi M, Carrasquillo JA, Chen CC, Martiniova L, Whatley M, et al. The effects of carbidopa on uptake of 6-18F-Fluoro-L-DOPA in PET of pheochromocytoma and extraadrenal abdominal paraganglioma. J Nucl Med. 2007;48:1599–606.
- Luxen A, Perlmutter M, Bida GT, Van Moffaert G, Cook JS, Satyamurthy N, et al. Remote, semiautomated production of 6-[18F]fluoro-L-dopa for human studies with PET. Int J Rad Appl Instrum A. 1990;41:275–81.
- Namavari M, Bishop A, Satyamurthy N, Bida G, Barrio JR. Regioselective radiofluorodestannylation with [18F]F2 and [18F]CH3COOF: a high yield synthesis of 6-[18F]Fluoro-L-dopa. Int J Rad Appl Instrum A. 1992;43:989–96.
- Vernaleken I, Kumakura Y, Cumming P, Buchholz HG, Siessmeier T, Stoeter P, et al. Modulation of [18F]fluorodopa (FDOPA) kinetics in the brain of healthy volunteers after acute haloperidol challenge. Neuroimage. 2006;30:1332–9.
- Garnett S, Firnau G, Nahmias C, Chirakal R. Striatal dopamine metabolism in living monkeys examined by positron emission tomography. Brain Res. 1983;280:169–71.
- Beheshti M, Pocher S, Vali R, Waldenberger P, Broinger G, Nader M, et al. The value of 18F-DOPA PET-CT in patients with medullary thyroid carcinoma: comparison with 18F-FDG PET-CT. Eur Radiol. 2009;19:1425–34.
- Soussan M, Nataf V, Kerrou K, Grahek D, Pascal O, Talbot JN, et al. Added value of early 18F-FDOPA PET/CT acquisition time in medullary thyroid cancer. Nucl Med Commun. 2012;33:775–9.

- Ginet M, Cuny T, Schmitt E, Marie PY, Verger A. 18F-FDOPA PET Imaging in Prolactinoma. Clin Nucl Med. 2017;42:e383

 –e4.
- 115. Berends AMA, Kerstens MN, Bolt JW, Links TP, Korpershoek E, de Krijger RR, et al. False-positive findings on 6-[18F]fluor-l-3,4-dihydroxyphenylalanine PET ((18)F-FDOPA-PET) performed for imaging of neuroendocrine tumours. Eur J Endocrinol. 2018;179: 127–35
- 116. Treglia G, Cocciolillo F, de Waure C, Di Nardo F, Gualano MR, Castaldi P, et al. Diagnostic performance of 18F-dihydroxyphenylalanine positron emission tomography in patients with paraganglioma: a meta-analysis. Eur J Nucl Med Mol Imaging. 2012;39:1144–53.
- 117. Charrier N, Deveze A, Fakhry N, Sebag F, Morange I, Gaborit B, et al. Comparison of [(1)(1)(1)In]pentetreotide-SPECT and [(1)F]FDOPA-PET in the localization of extra-adrenal paragangliomas: the case for a patient-tailored use of nuclear imaging modalities. Clin Endocrinol. 2011;74:21–9.
- Fanti S, Ambrosini V, Tomassetti P, Castellucci P, Montini G, Allegri V, et al. Evaluation of unusual neuroendocrine tumours by means of 68Ga-DOTA-NOC PET. Biomed Pharmacother. 2008;62:667–71.
- Hoegerle S, Ghanem N, Altehoefer C, Schipper J, Brink I, Moser E, et al. 18F-DOPA positron emission tomography for the detection of glomus tumours. Eur J Nucl Med Mol Imaging. 2003;30: 689–94.
- King KS, Whatley MA, Alexopoulos DK, Reynolds JC, Chen CC, Mattox DE, et al. The use of functional imaging in a patient with head and neck paragangliomas. J Clin Endocrinol Metab. 2010;95:481–2.
- Hoegerle S, Nitzsche E, Altehoefer C, Ghanem N, Manz T, Brink I, et al. Pheochromocytomas: detection with 18F DOPA whole body PET-initial results. Radiology. 2002;222:507–12.
- Imani F, Agopian VG, Auerbach MS, Walter MA, Imani F, Benz MR, et al. 18F-FDOPA PET and PET/CT accurately localize pheochromocytomas. J Nucl Med. 2009;50:513–9.
- 123. Kauhanen S, Seppanen M, Ovaska J, Minn H, Bergman J, Korsoff P, et al. The clinical value of [18F]fluoro-dihydroxyphenylalanine positron emission tomography in primary diagnosis, staging, and restaging of neuroendocrine tumours. Endocr Relat Cancer. 2009;16:255–65.
- 124. Luster M, Karges W, Zeich K, Pauls S, Verburg FA, Dralle H, et al. Clinical value of 18F-fluorodihydroxyphenylalanine positron emission tomography/computed tomography (18F-DOPA PET/ CT) for detecting pheochromocytoma. Eur J Nucl Med Mol Imaging. 2010;37:484–93.
- 125. Rischke HC, Benz MR, Wild D, Mix M, Dumont RA, Campbell D, et al. Correlation of the Genotype of Paragangliomas and Pheochromocytomas with Their Metabolic Phenotype on 3,4-di-hydroxy-6-18F-fluoro-L-phenylalanin PET. J Nucl Med. 2012;53: 1352–8.
- 126. Nambuba J, Darr R, Janssen I, Bullova P, Adams KT, Millo C, et al. Functional imaging experience in a germline fumarate hydratase mutation–positive patient with pheochromocytoma and paraganglioma. AACE Clin Case Rep. 2016;2:e176–e81.
- Burnichon N, Vescovo L, Amar L, Libe R, de Reynies A, Venisse A, et al. Integrative genomic analysis reveals somatic mutations in pheochromocytoma and paraganglioma. Hum Mol Genet. 2011;20:3974–85.
- Favier J, Briere JJ, Burnichon N, Riviere J, Vescovo L, Benit P, et al. The Warburg effect is genetically determined in inherited pheochromocytomas. PLoS One. 2009;4:e7094.
- Lopez-Jimenez E, Gomez-Lopez G, Leandro-Garcia LJ, Munoz I, Schiavi F, Montero-Conde C, et al. Research resource: transcriptional profiling reveals different pseudohypoxic signatures in SDHB and VHL-related pheochromocytomas. Mol Endocrinol. 2010;24:2382–91.



- 130. Pollard PJ, El-Bahrawy M, Poulsom R, Elia G, Killick P, Kelly G, et al. Expression of HIF-1alpha, HIF-2alpha (EPAS1), and their target genes in paraganglioma and pheochromocytoma with VHL and SDH mutations. J Clin Endocrinol Metab. 2006;91:4593–8.
- 131. Span PN, Rao JU, Oude Ophuis B, Lenders JW, Sweep F, Wesseling P, et al. Overexpression of the natural antisense hypoxia-inducible factor-lalpha transcript is associated with malignant phaeochromocytoma/paraganglioma. Endocr Relat Cancer. 2011.
- 132. Taieb D, Sebag F, Barlier A, Tessonnier L, Palazzo FF, Morange I, et al. 18F-FDG avidity of pheochromocytomas and paragangliomas: a new molecular imaging signature? J Nucl Med. 2009:50:711-7.
- Garrigue P, Bodin-Hullin A, Balasse L, Fernandez S, Essamet W, Dignat-George F, et al. The Evolving Role of Succinate in Tumour Metabolism: An (18)F-FDG-Based Study. J Nucl Med. 2017;58: 1749–55.
- 134. Taieb D, Pacak K. New Insights into the Nuclear Imaging Phenotypes of Cluster 1 Pheochromocytoma and Paraganglioma. Trends Endocrinol Metab. 2017;28:807–17.
- Boellaard R, Delgado-Bolton R, Oyen WJ, Giammarile F, Tatsch K, Eschner W, et al. FDG PET/CT: EANM procedure guidelines for tumour imaging: version 2.0. Eur J Nucl Med Mol Imaging. 2015;42:328–54.
- ICRP. Radiation Dose to Patients from Radiopharmaceuticals -Addendum 3 to ICRP Publication 53. ICRP Publication 106. Approved by the Commission in October 2007. Ann IRCP. 2008;38:1–197.
- Zanotti-Fregonara P, Jan S, Taieb D, Cammilleri S, Trebossen R, Hindie E, et al. Absorbed 18F-FDG dose to the fetus during early pregnancy. J Nucl Med. 2010;51:803–5.
- Zanotti-Fregonara P, Chastan M, Edet-Sanson A, Ekmekcioglu O, Erdogan EB, Hapdey S, et al. New fetal doses from 18FDG administered during pregnancy: standardization of dose calculations and estimations with voxel-based anthropomorphic phantoms. J Nucl Med. 2016;57:1760–3.
- Guerin C, Pattou F, Brunaud L, Lifante JC, Mirallie E, Haissaguerre M, et al. Performance of 18F-FDG PET/CT in the Characterization of Adrenal Masses in Noncancer Patients: A Prospective Study. J Clin Endocrinol Metab. 2017;102:2465–72.
- 140. Timmers HJ, Chen CC, Carrasquillo JA, Whatley M, Ling A, Eisenhofer G, et al. Staging and functional characterization of pheochromocytoma and paraganglioma by 18F-fluorodeoxyglucose (18F-FDG) positron emission tomography. J Natl Cancer Inst. 2012;104:700–8.
- 141. Timmers HJ, Kozupa A, Chen CC, Carrasquillo JA, Ling A, Eisenhofer G, et al. Superiority of fluorodeoxyglucose positron emission tomography to other functional imaging techniques in the evaluation of metastatic SDHB-associated pheochromocytoma and paraganglioma. J Clin Oncol. 2007;25:2262–9.
- Tiwari A, Shah N, Sarathi V, Malhotra G, Bakshi G, Prakash G, et al. Genetic status determines (18) F-FDG uptake in pheochromocytoma/paraganglioma. J Med Imaging Radiat Oncol. 2017;61:745–52.
- 143. Gabriel M, Decristoforo C, Donnemiller E, Ulmer H, Watfah Rychlinski C, Mather SJ, et al. An intrapatient comparison of 99mTc-EDDA/HYNIC-TOC with 111In-DTPA-octreotide for diagnosis of somatostatin receptor-expressing tumours. J Nucl Med. 2003;44:708–16.
- Grimes J, Celler A, Birkenfeld B, Shcherbinin S, Listewnik MH, Piwowarska-Bilska H, et al. Patient-specific radiation dosimetry of 99mTc-HYNIC-Tyr3-octreotide in neuroendocrine tumours. J Nucl Med. 2011;52:1474–81.
- 145. Pacak K, Eisenhofer G, Carrasquillo JA, Chen CC, Li ST, Goldstein DS. 6-[18F]fluorodopamine positron emission

- tomographic (PET) scanning for diagnostic localization of pheochromocytoma. Hypertension. 2001;38:6–8.
- 146. Ilias I, Yu J, Carrasquillo JA, Chen CC, Eisenhofer G, Whatley M, et al. Superiority of 6-[18F]-fluorodopamine positron emission tomography versus [131I]-metaiodobenzylguanidine scintigraphy in the localization of metastatic pheochromocytoma. J Clin Endocrinol Metab. 2003;88:4083–7.
- 147. Mann GN, Link JM, Pham P, Pickett CA, Byrd DR, Kinahan PE, et al. [11C]metahydroxyephedrine and [18F]fluorodeoxyglucose positron emission tomography improve clinical decision making in suspected pheochromocytoma. Ann Surg Oncol. 2006;13:187–97
- 148. Shulkin BL, Wieland DM, Schwaiger M, Thompson NW, Francis IR, Haka MS, et al. PET scanning with hydroxyephedrine: an approach to the localization of pheochromocytoma. J Nucl Med. 1992;33:1125–31.
- Trampal C, Engler H, Juhlin C, Bergstrom M, Langstrom B. Pheochromocytomas: detection with 11C hydroxyephedrine PET. Radiology. 2004;230:423–8.
- Franzius C, Hermann K, Weckesser M, Kopka K, Juergens KU, Vormoor J, et al. Whole-body PET/CT with 11C-metahydroxyephedrine in tumours of the sympathetic nervous system: feasibility study and comparison with 123I-MIBG SPECT/CT. J Nucl Med. 2006;47:1635–42.
- 151. Rahbar K, Kies P, Stegger L, Juergens KU, Weckesser M. Discrepancy between glucose metabolism and sympathetic nerve terminals in a patient with metastatic paraganglioma. Eur J Nucl Med Mol Imaging. 2008;35:687.
- Loc'h C, Mardon K, Valette H, Brutesco C, Merlet P, Syrota A, et al. Preparation and pharmacological characterization of [76Br]meta-bromobenzylguanidine ([76Br]MBBG). Nucl Med Biol. 1994;21:49–55.
- Vaidyanathan G, Affleck DJ, Zalutsky MR. Validation of 4-[fluorine-18]fluoro-3-iodobenzylguanidine as a positron-emitting analog of MIBG. J Nucl Med. 1995;36:644–50.
- 154. Yu M, Bozek J, Lamoy M, Guaraldi M, Silva P, Kagan M, et al. Evaluation of LMI1195, a novel 18F-labeled cardiac neuronal PET imaging agent, in cells and animal models. Circ Cardiovasc Imaging. 2011;4:435–43.
- 155. Pandit-Taskar N, Zanzonico P, Staton KD, Carrasquillo JA, Reidy-Lagunes D, Lyashchenko S, et al. Biodistribution and Dosimetry of (18)F-Meta-Fluorobenzylguanidine: A First-in-Human PET/CT Imaging Study of Patients with Neuroendocrine Malignancies. J Nucl Med. 2018;59:147–53.
- 156. Martiniova L, Perera SM, Brouwers FM, Alesci S, Abu-Asab M, Marvelle AF, et al. Increased uptake of [(1)(2)(3)I]meta-iodobenzylguanidine, [(1)F]fluorodopamine, and [(3)H]norepinephrine in mouse pheochromocytoma cells and tumors after treatment with the histone deacetylase inhibitors. Endocr Relat Cancer. 2011;18:143–57.
- Taieb D, Neumann H, Rubello D, Al-Nahhas A, Guillet B, Hindie E. Modern nuclear imaging for paragangliomas: beyond SPECT. J Nucl Med. 2012;53:264

 –74.
- Taieb D, Rubello D, Al-Nahhas A, Calzada M, Marzola MC, Hindie E. Modern PET imaging for paragangliomas: relation to genetic mutations. Eur J Surg Oncol. 2011;37:662–8.
- Havekes B, King K, Lai EW, Romijn JA, Corssmit EP, Pacak K. New imaging approaches to phaeochromocytomas and paragangliomas. Clin Endocrinol. 2010;72:137–45.
- Taieb D, Timmers HJ, Hindie E, Guillet BA, Neumann HP, Walz MK, et al. EANM 2012 guidelines for radionuclide imaging of phaeochromocytoma and paraganglioma. E. Eur J Nucl Med Mol Imaging. 2012;39:1977–95.
- Hes FJ, Weiss MM, Woortman SA, de Miranda NF, van Bunderen PA, Bonsing BA, et al. Low penetrance of a SDHB mutation in a large Dutch paraganglioma family. BMC Med Genet. 2010;11:92.



- 162. Schiavi F, Milne RL, Anda E, Blay P, Castellano M, Opocher G, et al. Are we overestimating the penetrance of mutations in SDHB? Hum Mutat. 2010;31:761–2.
- Solis DC, Burnichon N, Timmers HJ, Raygada MJ, Kozupa A, Merino MJ, et al. Penetrance and clinical consequences of a gross SDHB deletion in a large family. Clin Genet. 2009;75:354–63.
- 164. Rijken JA, Niemeijer ND, Jonker MA, Eijkelenkamp K, Jansen JC, van Berkel A, et al. The penetrance of paraganglioma and pheochromocytoma in SDHB germline mutation carriers. Clin Genet. 2018;93:60–6.
- 165. Andrews KA, Ascher DB, Pires DEV, Barnes DR, Vialard L, Casey RT, et al. Tumour risks and genotype-phenotype correlations associated with germline variants in succinate dehydrogenase subunit genes SDHB, SDHC and SDHD. J Med Genet. 2018;55:384–94.
- 166. Heesterman BL, de Pont LMH, van der Mey AG, Bayley JP, Corssmit EP, Hes FJ, et al. Clinical progression and metachronous

- paragangliomas in a large cohort of SDHD germline variant carriers. Eur J Hum Genet. 2018;26:1339–47.
- 167. Lepoutre-Lussey C, Caramella C, Bidault F, Deandreis D, Berdelou A, Al Ghuzlan A, et al. Screening in asymptomatic SDHx mutation carriers: added value of (1)(8)F-FDG PET/CT at initial diagnosis and 1-year follow-up. Eur J Nucl Med Mol Imaging. 2015;42:868–76.
- 168. Daniel E, Jones R, Bull M, Newell-Price J. Rapid-sequence MRI for long-term surveillance for paraganglioma and phaeochromocytoma in patients with succinate dehydrogenase mutations. Eur J Endocrinol. 2016;175:561–70.

Publisher's note Springer Nature remains neutral with regard to jurisdictional claims in published maps and institutional affiliations.

